Photosystem II

DOI: 10.1002/anie.200600917

The Possible Role of Proton-Coupled Electron Transfer (PCET) in Water Oxidation by Photosystem II

Thomas J. Meyer, My Hang V. Huynh, and H. Holden Thorp*

Keywords:
coupled electron–proton transfer · electron transfer · photosynthesis · photosystem II · proton transport

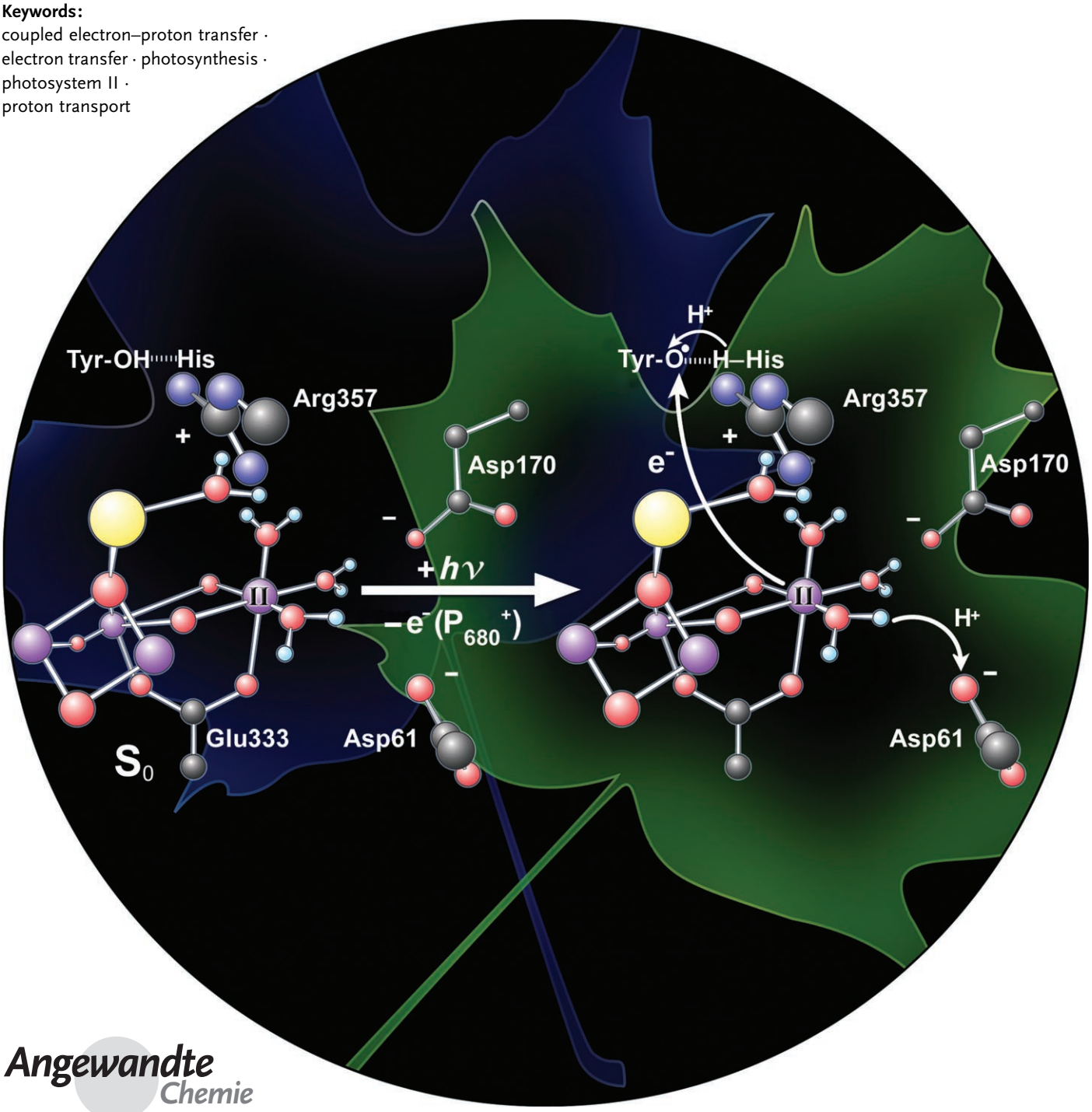

All higher life forms use oxygen and respiration as their primary energy source. The oxygen comes from water by solar-energy conversion in photosynthetic membranes. In green plants, light absorption in photosystem II (PSII) drives electron-transfer activation of the oxygen-evolving complex (OEC). The mechanism of water oxidation by the OEC has long been a subject of great interest to biologists and chemists. With the availability of new molecular-level protein structures from X-ray crystallography and EXAFS, as well as the accumulated results from numerous experiments and theoretical studies, it is possible to suggest how water may be oxidized at the OEC. An integrated sequence of light-driven reactions that exploit coupled electron–proton transfer (EPT) could be the key to water oxidation. When these reactions are combined with long-range proton transfer (by sequential local proton transfers), it may be possible to view the OEC as an intricate structure that is "wired for protons".

From the Contents

1. Introduction

Photosystem II (PSII) is a multi-polypeptide complex found in thylakoid membranes of chloroplasts in plants and algae. It uses water as the electron donor in the photochemical oxidation of water to dioxygen as shown in Equation (1). In green plants, the electrons created in this

$$2\,H_2O + 4\,h\nu \rightarrow O_2 + 4\,e^- + 4\,H^+ \quad (1)$$

reaction reduce a benzoquinone to hydroquinone and transfer reductive equivalents to photosystem I, where they enter the Calvin cycle for reduction of CO_2.[1–15]

Recent advances, especially the results of X-ray structures of PSII from cyanobacterium *Thermosynechococcus elongates* at 3-Å and 3.5-Å resolution, have given insight at the molecular level into how O_2 is formed in PSII.[16–23]

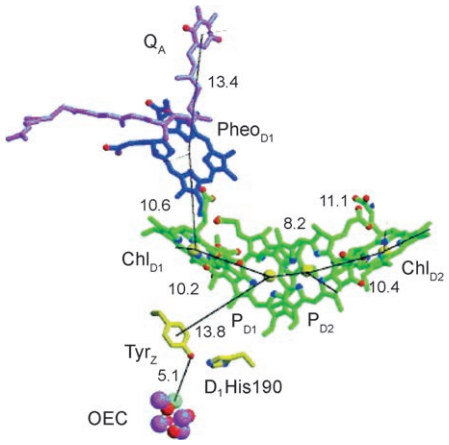

Figure 1. Molecular structure of the reaction center of photosystem II from cyanobacterium *Thermosynechococcus elongates* illustrating the Tyr_Z-Chl_{D1}(P_{680})-$Pheo_{D1}$-Q_A donor–chromophore–acceptor (D–C–A) array and the proximity of Tyr_Z to the oxygen-evolving complex (OEC); blue: pheophytin, dark green: chlorophyll, yellow: Y_Z, light green: Ca, purple: Mn. Reproduced from reference [16].

It is known that oxygen is evolved after the sequential absorption of four photons (Kok cycle).[24] The recent structures reinforce earlier suggestions that each cycle is initiated by sensitization of chlorophyll P_{680} (Chl_{D1} in Figure 1), followed by rapid electron transfer through intervening pheophytin D_1 ($Pheo_{D1}$) to benzoquinone acceptor Q_A.

The oxidized chlorophyll, P_{680}^+, subsequently oxidizes tyrosine Tyr_Z by long-range (ca. 10 Å) electron transfer to give $Tyr_Z^{\bullet}$. As discussed in Section 6, electron transfer appears to be coupled with proton transfer to D1Histidine 190. Thus, the light-driven sequence leads to the net reaction in Equation (2) with $Y_Z = Tyr_Z$-OH···His 190 and $Y_Z^{\bullet} = Tyr_Z$-O$^{\bullet}$···$^+$H-His 190.

$$Q_A\text{–}P_{680}\text{-}Y_Z \xrightarrow{h\nu} Q_A^-\text{-}P_{680}\text{-}Y_Z^{\bullet} \quad (2)$$

Water oxidation occurs at the oxygen-evolving complex (OEC) after it is oxidatively activated by $Y_Z^{\bullet}$.[1–3,16,19,20,25–39] The O_2/H_2O half reaction poses a major mechanistic chal-

[*] Prof. Dr. T. J. Meyer, Prof. Dr. H. H. Thorp
Department of Chemistry
University of North Carolina at Chapel Hill
Chapel Hill, NC 27599 (USA)
Fax: (+1) 919-962-2388
E-mail: tjmeyer@unc.edu
Dr. M. H. V. Huynh
Dynamic Materials Properties &
Energetic Materials Science Division
High Explosive Science and Technology Group
Los Alamos National Laboratory
Los Alamos, NM 87545 (USA)

lenge: it requires the loss of $4e^-$ and $4H^+$ in combination with O···O coupling.

In the Kok cycle, it is proposed that each of four sequential photons absorbed in PSII results in the loss of an electron, ultimately with the evolution of O_2.[24] Recent advances in experiment and theory enable insight into how this coupling may occur. The goal of this Review is to suggest a possible mechanism for water oxidation in which electron–proton coupling and proton transfer play central roles at three of the four stages of the Kok cycle. In view of the lack of definitive, high-resolution structural information, this mechanism is necessarily speculative. Its evolution has greatly benefited from the results of earlier analyses. The importance of proton involvement[40,41] and of the coupling of electrons and protons were developed as themes in earlier publications.[1,2,4,7,42] Also, mechanisms for water oxidation at the OEC have been proposed by a number of groups over a period of many years.[7,9,21,28,29,32,42–52]

2. Reaction Pathways for Coupled Electron–Proton Transfer

Comparisons of reaction rates, isotope effect measurements, and theory have led to the suggestion that the reactions in Equations (3),[53,54] (4),[55,56] and 5[57] all occur by redox (net e^- transfer) pathways that involve the simultaneous transfer of electrons and protons. They can be described as electron–proton transfer or EPT pathways.

$$cis\text{-}[Ru^{IV}(bpy)_2(py)(O)]^{2+} + cis\text{-}[Ru^{II}(bpy)_2(py)(H_2O)]^{2+} \rightarrow 2\,cis\text{-}[Ru^{III}(bpy)_2(py)(OH)]^{2+} \quad (3)$$

$$[Fe^{II}(H_2bim)_3]^{2+} + [Fe^{III}(Hbim)(H_2bim)_2]^{2+} \rightarrow [Fe^{III}(Hbim)(H_2bim)_2]^{2+} + [Fe^{II}(H_2bim)_3]^{2+} \quad (4)$$

$$PhOH + PhO^{\cdot} \rightarrow PhO^{\cdot} + PhOH \quad (5)$$

In this context, EPT is defined as a redox pathway or elementary step in which electrons and protons are transferred from different orbital sites on a donor to different orbital sites on an acceptor. Simultaneous or concerted means rapid relative to timescales for coupled vibrations (ca. 10 fs) and collective solvent modes (0.2–20 ps).

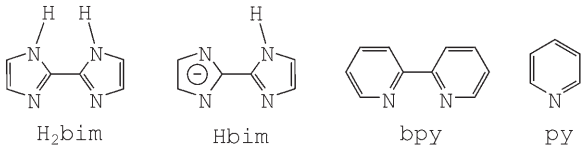

As shown in Equations (6)–(8) for the comproportionation reaction in Equation (3), these reactions are predicted to

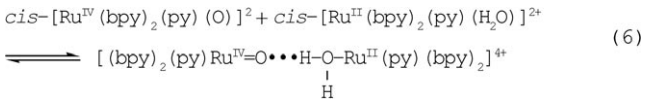

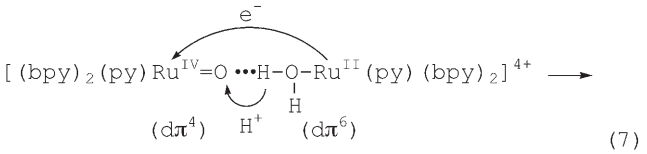

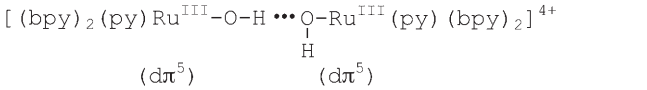

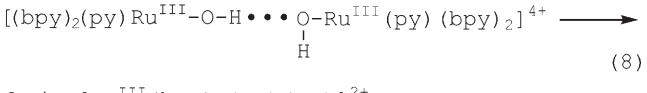

occur through preliminary H-bond formation because of the short-range nature of proton transfer.[58–68] In this example, electron transfer occurs between dπ orbitals (t_{2g} in O_h symmetry) largely centered at Ru^{II} and Ru^{IV}, and proton transfer occurs from a σ(O–H) orbital to an acceptor lone pair on the oxido group.

The EPT terminology is necessary to distinguish this pathway or elementary step from: 1) the class of net reactions, such as that in Equation (3), in which there is a change in proton content between reactants and products. This class of reactions has come to be called proton-coupled electron

Thomas J. Meyer received his BS degree at Ohio University, his PhD at Stanford with Henry Taube, and was a NATO postdoctoral fellow at University College, London, with Sir Ronald Nyholm in 1967. He joined the chemistry faculty at the University of North Carolina (UNC) at Chapel Hill and from 1994 to 1999 served as Vice Chancellor for Graduate Studies and Research. After a hiatus as Associate Director for Strategic Research at the Los Alamos National Laboratory he rejoined the faculty of UNC in 2005 as Arey Professor of chemistry. He is a member of the US National Academy of Sciences and American Academy of Arts and Sciences.

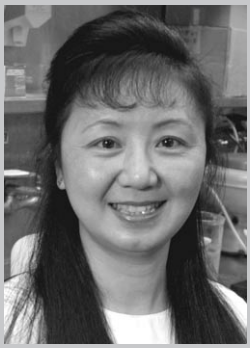

My Hang V. Huynh received her BS in chemistry and BA in Mathematics from the State University of New York at Geneseo with David K. Geiger and her PhD from the State University of New York at Buffalo with Kenneth J. Takeuchi. She carried out postdoctoral work at UNC at Chapel Hill and the Los Alamos National Laboratory (LANL) in New Mexico. Her current research at LANL on the chemistry of nitrogen-rich compounds focuses on the syntheses and applications of new organic and inorganic primary and secondary explosives. She recently received the E. O. Lawrence Award in Chemistry.

transfer (PCET); 2) mechanisms that occur by sequential electron transfer (ET) with subsequent proton transfer (PT) or vice versa; and 3) pathways in which electrons and protons come from the same chemical bond, such as in H-atom transfer (HAT)[69–77] or hydride transfer.[78–82]

There are also hybrid pathways in which one partner undergoes EPT and the other HAT or hydride transfer.[83] An example is the oxidation of formate anion by *cis*-$[Ru^{IV}(bpy)_2(py)(O)]^{2+}$ (*cis*-$[Ru^{IV}(bpy)_2(py)(O)]^{2+} + HCO_2^- \rightarrow$ *cis*-$[Ru^{II}(bpy)_2(py)(OH)]^+ + CO_2$), in which hydride transfer occurs from HCO_2^- to $Ru^{IV}{=}O$.[78]

As illustrated by reduction of the triplet excited state of C_{60} ($^3C_{60}$) by phenols with added N bases [Eqs. (9)–(11) with

$$^3C_{60} + ArO{-}H\cdots py \rightleftharpoons {}^3C_{60},ArO{-}H\cdots py \quad (9)$$

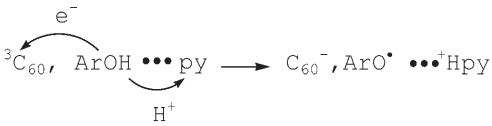

(10)

$$C_{60}^-,ArO^{\cdot}\cdots {}^+H{-}py \rightleftharpoons C_{60}^- + {}^{\cdot}ArO + {}^+H{-}py \quad (11)$$

pyridine (py) as the base], there is a second class of EPT pathways in which different sites play the role of electron ($^3C_{60}$) and proton (py) donor or acceptor.[84–86] Because more than one site is involved, such pathways can be described as multiple-site electron–proton transfer (MS-EPT), in which: 1) an electron–proton donor transfers electrons and protons to different acceptors or 2) an electron–proton acceptor accepts electrons and protons from different donors.[83]

As discussed in the next section, MS-EPT pathways, and EPT in general, are more complex than ET or PT. MS-EPT competes with sequential ET-PT or PT-ET mechanisms by avoiding high-energy intermediates. As an example, oxidation of tyrosine (Tyr-OH) as the phenol by ET in the first step of an ET-PT mechanism ($^3C_{60} + ArOH \rightarrow C_{60}^- + ArOH^{+\bullet}$) is unfavorable because of the high potential of the Tyr-$OH^{+\bullet}$/Tyr-OH couple (E^o(Tyr-$OH^{+\bullet}$/Tyr-OH) = 1.34 V vs NHE). By comparison, MS-EPT with pyridine as the proton acceptor ($^3C_{60} + ArOH + py \rightarrow C_{60}^- + ArO^{\bullet} + {}^+Hpy$) is more favorable by around 0.51 eV. Similarly, in a PT-ET mechanism, $\Delta G^o = +0.30$ eV for initial PT (Tyr-OH + py $\rightarrow$ Tyr-O^- + Hpy^+). In general, all three mechanisms may be operative and can be distinguished by kinetic measurements.

Holden Thorp received his undergraduate degree in chemistry at the UNC in Chapel Hill with Thomas J. Meyer and completed his PhD on the photochemistry of trans-dioxidorhenium(V) at Caltech with Harry B. Gray. He conducted postdoctoral work at Yale University with Gary W. Brudvig and Robert Crabtree on the redox chemistry of oxidomanganese clusters related to photosystem II. His research in Chapel Hill focuses on the redox chemistry and modification of nucleic acids. He is a Packard Fellow for Science and Engineering and an Alfred P. Sloan Fellow and was recently named Dean of the College of Arts and Sciences at UNC.

3. Theory of Coupled Electron–Proton Transfer

The theory of EPT for the generalized elementary step in Equation (12), in which D_{ox} is the oxidized form of the donor

(12)

and A_{red} the reduced form of the acceptor, has been developed in a series of papers by Cukier,[87–93] and Hammes-Schiffer and their co-workers,[56,94–107] as well as by others.[108–110] The theory developed by Hammes-Schiffer has proven to be especially useful in understanding relative rate constants, solvent effects, kinetic isotope effects, and other parameters. Electron-transfer theory provides a starting point, and proton transfer is included as a quantized, coupled high- or medium-frequency vibrational mode ν(E-H). In the treatment by Hammes-Schiffer and co-workers, strong electronic coupling between initial and final ν(E-H) vibrational states gives rise to a new set of adiabatic, proton-coupled states.

Electronic coupling is treated as in electron-transfer theory as an electrostatic perturbation that leads to donor–acceptor electronic wave function mixing. The resulting resonance energy, the electron-transfer matrix element V_{ET}, is given by Equation (13) in which ψ_A and ψ_D are the electronic wave functions for the acceptor and donor orbitals, respectively, and $\boldsymbol{H}$ is the operator mixing the states.

$$V_{ET} = \langle \psi_A | \boldsymbol{H} | \psi_D \rangle \quad (13)$$

Application of time-dependent perturbation theory gives the expression for the EPT rate constant k_{EPT} in Equation (14). The summations are over a series of vibrational

$$k_{EPT} = \frac{2\pi}{\hbar\sqrt{4\pi\lambda_{\mu\nu}\,k_B\,T}} \sum_{\mu} P_{I\mu} \sum_{\nu} |V_{\mu\nu}|^2 \exp\left(-\frac{(\Delta G_{\mu\nu} + \lambda)^2}{4\lambda_{\mu\nu}\,k_B\,T}\right) \quad (14)$$

channels from initial, coupled D–H···A vibrational levels μ to final D···H–A levels ν. The vibrational quantum spacing is $\hbar\omega$. $P_{I\nu}$ is the Boltzmann population in vibrational level μ in the initial state, D–H···A. $\lambda_{\mu\nu}$ is the classical reorganization energy for the $\mu \rightarrow \nu$ vibrational channel arising from the solvent and low-frequency modes. $V_{\mu\nu}$ is the EPT matrix element for the channel $\mu \rightarrow \nu$, and $\Delta G_{\mu\nu}$ is the free-energy change for this channel. It is related to ΔG_{EPT}, the overall free energy change for the EPT reaction, as shown in Equation (15). In Equa-

$$\Delta G_{\mu\nu} = \Delta G_{EPT} + (\mu - \nu)\hbar\omega \quad (15)$$

tion (14), the classical barrier crossing term $\exp(-(\Delta G_{\mu\nu}+\lambda)^2/4\lambda_{\mu\nu}k_B T)$ gives the population of molecules at temperature T at the classical barrier crossing for the solvent and for all coupled modes for the $\mu\rightarrow\nu$ channel except ν(E-H). The summation over ν typically involves a limited number of levels, those for which the barrier crossing term is minimized.

If the Condon approximation separating nuclear and electronic motion is valid, $V_{\mu\nu}$ is given by the product of a vibrational overlap integral and the electron-transfer matrix element [Eq. (16)]. If this approximation is not valid, the

$$V_{\mu\nu} \approx V_{ET}\langle\phi_\mu^I|\phi_\nu^{II}\rangle \quad (16)$$

coordinates of the exchanging electron and proton are mixed. In Equation (16), ϕ_μ^I and ϕ_ν^{II} are the proton ν(E-H) vibrational wave functions for the adiabatic, mixed initial and final proton states, respectively. The square of the vibrational overlap integral $\langle\phi_\mu^I|\phi_\nu^{II}\rangle^2$ gives a quantitative measure of the extent to which the reactants and products coexist spatially along the proton-transfer coordinate. A transition between vibrational levels is referred to as nuclear tunneling in the physics literature. It is a quantum effect arising from the probabilistic uncertainty in spatial coordinates for particles at the atomic level.

Changes in proton equilibrium displacement in either proton transfer or EPT are large relative to, for example, changes in displacement for coupled vibrations in electron transfer or excited-state decay. This leads to small vibrational overlaps with $\langle\phi_\mu^I|\phi_\nu^{II}\rangle \ll 1$. In this limit, barrier-crossing dynamics for an individual vibrational channel are dictated by the product $V_{ET}\langle\phi_\mu^I|\phi_\nu^{II}\rangle$. Even if V_{ET} is large, the product is small, and the preexponential terms for EPT through channel $\mu\rightarrow\nu$ is given by Equation (17).

$$\nu_{EPT,\mu\nu} = \frac{2\pi}{\hbar\sqrt{4\pi\lambda_{\mu\nu}k_B T}} V_{ET}^2\langle\phi_\mu^I|\phi_\nu^{II}\rangle^2 \quad (17)$$

From the expression for the de Broglie wavelength $\lambda = h/(2mE)^{1/2}$ and the masses of the electron and proton, the proton wavelength at a fixed energy is less extended than the electron wavelength by approximately 40 for the proton and by approximately 60 for the deuteron. Because of this, vibrational wave functions decrease far more rapidly with distance than electronic wave functions. The distances required for significant vibrational wave function overlap are much smaller than those for electronic wave function overlap. Even small changes in proton-transfer distance can lead to large changes in $\langle\phi_\mu^I|\phi_\nu^{II}\rangle$, and they can impact k_{EPT} significantly. It follows that the distance dependence of EPT is dominated by proton transfer because of its short-range nature. This includes PSII, for which proton transfer and EPT are key elements for catalytic water oxidation.

Because of the short-range nature of EPT and proton transfer, structural features (such as prior H-bond formation) that minimize proton-transfer distances and maximize vibrational overlap are required. Of necessity, long-range proton transfers occur by a series of discrete, quantized local proton-transfer steps driven by free energy or concentration gradients. Meeting the demands for EPT and sequential proton transfers over a distance imposes significant local structural requirements. The intricate way in which these requirements appear to be met in PSII for EPT and sequential proton transfer introduces the concept of "proton wiring".

4. PCET and EPT in Photosystem II: Thermodynamics

MS-EPT and EPT pathways are more demanding than individual PT or ET pathways because of the combined orbital requirements for simultaneous proton and electron transfer to occur. As noted in Section 3, EPT competes by avoiding high-energy intermediates, which greatly decrease rates when they appear as part of a redox mechanism.

These considerations are directly relevant to water oxidation in PSII. The individual steps in the Kok cycle, and activation of the OEC toward water oxidation, are initiated by P_{680}^+ oxidation of tyrosine Y_Z by long-range (ca. 10 Å) electron transfer to give $Y_Z^\bullet$ (Figure 1 and Equation (2)). In a recently revised estimate, the redox potential for the $P_{680}^{+/0}$ redox couple was given as $E^{o\prime}(P_{680}^{+/0}) = 1.26$ V (vs NHE).[111] With this value, as well as the values $E^{o\prime}(\text{Tyr-OH}^{+\bullet/0}) = 1.34$ V vs NHE, $pK_a(\text{Tyr-OH}^{+\bullet}) = -2$, $pK_a(\text{Tyr-OH}) = 10$, and $pK_a(^+\text{H-His}) = 5.5$, the driving forces for electron transfer (ET), electron–proton transfer (MS-EPT), and proton transfer (PT) at Tyr 161 are compared in Equations (18)–(20). The change in ΔG for MS-EPT was calculated from $\Delta G_{EPT}^o(\text{eV}, 25\,^\circ\text{C}) = -(F(E^o(P_{680}^{+/0}) - E^o(\text{Tyr-OH}^{+\bullet/0}))) - 0.059(pK_a(^+\text{H-His}) - pK_a(\text{Tyr-OH}^{+\bullet}))$, and that for PT from $\Delta G_{PT}^o = -0.059(pK_a(^+\text{H-His}) - pK_a(\text{Tyr-OH}))$.[111–116] F is the Faraday constant, which is 1 eV/V in SI units.

The calculated values in Equations (18)–(20) do not include the difference in ΔG for forming the initial and final H-bonded adducts, which for MS-EPT are Tyr-O–H···His 190 and Tyr-O$^\bullet$···$^+$His 190. They are also solution values and only an approximation to the actual values in the photosynthetic membrane. However, they do illustrate the sometimes considerable energetic advantages that can exist for a mechanism involving EPT relative to initial ET or PT. As noted by Babcock and co-workers[1,2,4,7,26,27,39] and by Krishtalik,[117–119] this advantage may be essential in PSII to ensure rapid oxidation of Tyr_Z. Oxidation of Y_Z is in competition with back electron transfer between Q_A^- and P_{680}^+, which occurs within around 200 μs at room temperature.[120,121]

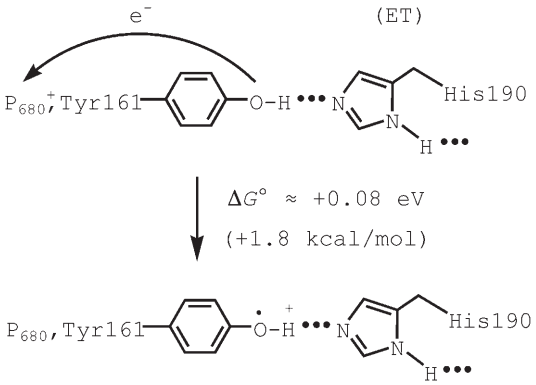

(18)

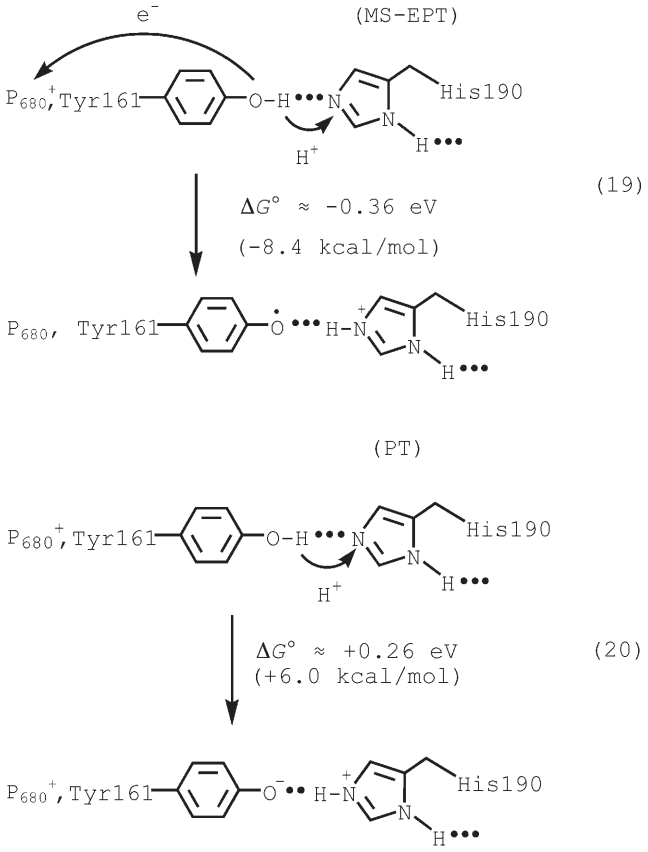

Experimental estimates place the potential for the $Y_Z^{\bullet}/Y_Z$ couple between 1.1 and 1.2 V. This value is considerably less than $E^{o\prime}$ for the Tyr-$OH^{+\bullet}$/Tyr-OH couple. The smaller value is consistent with formulating the $Y_Z^{\bullet}/Y_Z$ couple as Tyr-O$^{\bullet}\cdots{}^{+}$H-His190/Tyr-O–H$\cdots$His190 rather than Tyr-$OH^{+\bullet}$/Tyr-OH. With this interpretation, there is an increase in potential for the Tyr-O$^{\bullet}\cdots{}^{+}$H-His190/Tyr-O–H$\cdots$His190 couple from approximately 0.9 V in solution to 1.1–1.2 V in the photosynthetic membrane. The increase can be attributed largely to destabilization of the positive charge in the oxidized form of the couple in the relatively nonpolar membrane environment.

The standard potential for water oxidation at pH 7 [Eq. (21)] is 0.815 V (vs NHE), or 0.884 V when the free

$$O_2 + 4\,e^- + 4\,H^+ \rightarrow 2\,H_2O \qquad (21)$$

energy of dilution of O_2 is excluded, according to an analysis by Krishtalik.[117–119]

These potentials leave a narrow potential window for water oxidation by $Y_Z^{\bullet}$ and rule out high-energy intermediates such as $^{\bullet}$OH. Estimated reduction potentials for the S_1/S_0 and S_2/S_1 couples are 0.80 and 1.0 V, respectively.[122,123] Values for the other couples in the Kok cycle greatly in excess of the 1.1–1.2 V potential for the $Y_Z^{\bullet}/Y_Z$ couple would lead to high barriers for ET or EPT. The barriers in the operating OEC can not be too high, since activation energies for the individual S state transitions are low (between 0.05 and 0.4 eV for the $S_2 \rightarrow S_3$ transition).[124–128] The OEC turns over on the millisecond timescale.[2,27,129]

The need to avoid high-energy intermediates necessitates PCET and EPT in the Kok cycle. Oxidation without proton loss leads to an increase in positive charge. The buildup of charge in adjacent redox couples can lead to a significant increase in redox potentials. This occurs, for example, in the stepwise oxidation of a series of oxido and sulfido metal clusters, for which $E^{o\prime}$ increases by 0.3–0.4 V at each step.[32,130] By comparison, oxidation of *cis*-$[Ru^{II}(bpy)_2(H_2O)_2]^{2+}$ to *cis*-$[Ru^{VI}(bpy)_2(O)_2]^{2+}$ occurs at a single site by four sequential oxidations over a potential range of only 0.6 V. The narrow potential range and redox potential leveling are due to both PCET (coupled e^-/H^+ loss leads to no increase in charge) and stabilization of the higher oxidation states by Ru=O bond formation.[131–133]

5. Oxidation States and Structure

Results obtained by EPR and Mn X-ray absorption near edge spectroscopy (XANES) have been interpreted as favoring the oxidation-state distribution $Mn^{III}Mn^{III}Mn^{IV}Mn^{IV}$ for the S_1 state of the OEC.[134–140] This conclusion is in agreement with Kβ XES data[140,141] and with ^{55}Mn ENDOR spectra of PSII centers in the S_2 state.[142]

S_1 is the stable resting state in the dark.[21] The distribution $Mn^{II}Mn^{III}Mn^{IV}Mn^{IV}$ has been suggested for S_0,[9,21,135,136,143,144] although this formulation has been questioned recently on the basis of low-temperature electron-spin-lattice relaxation measurements.[145]

Recent X-ray diffraction (XRD) investigations on PSII at 3-[23] and 3.5-Å resolution[16] have provided molecular-level structural information about the OEC. Different views are shown in Figures 2, 3, and 6. Radiation damage and possible radiation-induced structural changes, disorder, and reduction of Mn^{III} and Mn^{IV} to Mn^{II} by X-ray generated radicals may complicate the interpretation of XRD results.[146–147]

The more-recent structure of the OEC at 3-Å resolution is shown in Figure 3.[23] Figure 2 is a modified version of one stereoview of the original 3.5-Å structure.[35] It has been modified to include possible coordination details around Ca and the Mn(3) and Mn(4) cluster sites, which is useful for the mechanistic discussion that follows.[35] There is no information in these structures about the water molecules shown coordinated to Mn(4). They are included because our PCET analysis points to these putative sites as critical in EPT and PT steps for oxidative activation of the OEC and water oxidation.

Other important features pertaining to mechanism appear in both structures, including: 1) the disposition of Tyr_z, and its associated histidine base relative to the OEC, 2) the existence of a $\{CaMn_3\}$ cluster at the core of the OEC, and 3) a structurally appended Mn(4) center, which lies near Asp170 and contains Asp61 in its second coordination sphere.

The structures in Figures 2 and 3 are related, but significant differences do appear in the higher resolution structure, such as the apparent bridging rather than terminal roles for Asp342, Glu189, and Glu333 as ligands and the binding of Ala344 to Mn(2) rather than Ca, which is consistent with FTIR results.

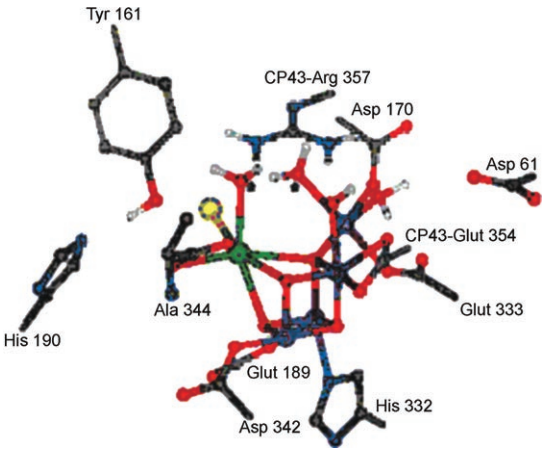

Figure 2. Structure of the PSII OEC from reference [16], modified as in reference [35]. C dark gray, O red, N dark blue, Mn purple, Ca green. Hydrogen atoms are not included in the published structure. Amino acid residues are numbered according to sequences in *Thermosynechoccus elongates*. The residues shown belong to the D_1 subunit of PSII with E354 belonging to CP43. Those bound to a Mn ion are shown as truncated side chains except for Ala 344, which is shown in its entirety. Two water ligands, not found in the structure but proposed as sites for O···O coupling, are each labeled with an asterisk.

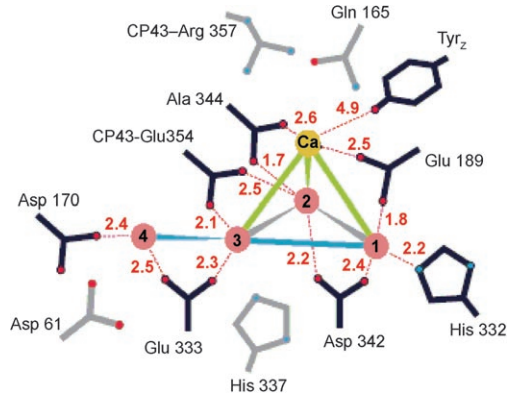

Figure 3. The {$CaMn_4$} cluster of the OEC with distances in Å taken from reference [23]. Ca orange, Mn pink, N blue, O red. The distances between Mn and Ca, as illustrated by the connecting lines, are: 2.7 (gray), 3.3 (blue), and 3.4 Å (green). Amino acids in black are in the first coordination sphere and those beyond are in gray.

From earlier EXAFS results on S_1, it was proposed that the OEC is composed of two to three di-μ-oxido Mn units with Mn···Mn separation distances of around 2.7 Å.[9,13,148–151] A recent extended range EXAFS study on S_1 revealed three Mn···Mn vectors in the {$CaMn_3$} cluster, two of around 2.7 Å and one of approximately 2.8 Å, as well as another one or two Mn···Mn interactions with a separation of 3.3 Å.[152]

Even more recently, the structure of S_1 was investigated by EXAFS measurements on single crystals free of radiation damage.[153] The EXAFS results were consistent with three different but topologically related structures for the OEC. The most favored structure, on the basis of the XRD data, is shown in Figure 4.

There are considerable differences in orientation and structure between Figure 3 and the favored EXAFS structure in Figure 4, but the basic cluster and ligand frameworks are retained in both. Notable features are di-μ-oxido bridging between each pair of Mn partners, a single tri-μ-oxido bridge between Ca and Mn(2) and Mn(3), and the long Mn(4)···O distance between Mn(4) and Asp 170.

A schematic drawing of the OEC based on the EXAFS structure in Figure 4 is shown in Figure 5. The important elements that will play a role in the following mechanistic discussion include:

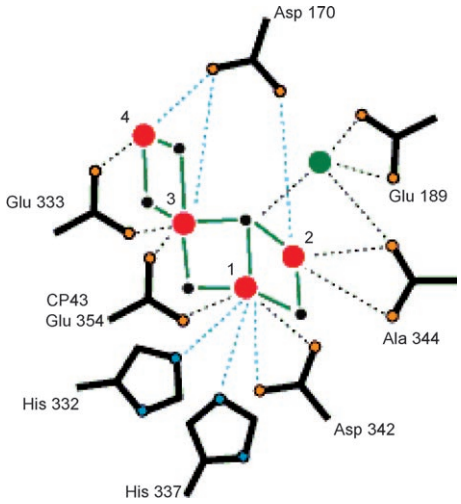

Figure 4. Structural diagram showing the favored EXAFS structure for the OEC in S_1. Ca green, Mn red, N blue, O orange. Mn–oxido bonds are shown as solid green lines. Bonds to other possible ligand atoms are shown as dotted lines; black: distances less than 3.0 Å, blue: distances greater than 3.0 Å. Reproduced in modified form from reference [153].

1) The coordinative stabilization of the Mn(4) center by triple bridging to the Mn(3) center.
2) The presence of three coordinated water molecules at Mn(4) in S_0, as well as two water molecules and a hydroxide ion in S_1. In the proposed mechanism all three play a role in the critical proton-transfer and EPT steps that result in oxidative activation and water oxidation. The coordinated water molecules are assumed but not established in the 3.0- or 3.5-Å structures.

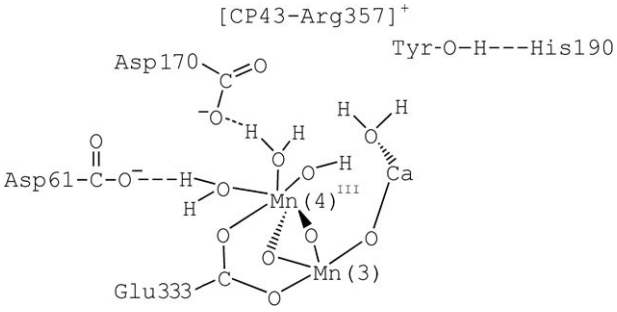

Figure 5. Possible structural features at the OEC, on the basis of the EXAFS and XRD structures in Figures 3 and 4. The water molecules shown are not observed in either the EXAFS or XRD structures.

3) The suggested H-bond interaction between Mn(4)-OH_2 and Asp61.
4) The suggestion that Asp170 is H-bonded to a coordinated water molecule rather than coordinated to the Mn(4) center.

6. MS-EPT in the Oxidative Activation of the OEC

6.1. Oxidation of Y_Z by P_{680}^+

In their initial formulation of coupled electron–proton transfer in PSII, Babcock and co-workers suggested an "H-abstraction" mechanism on the basis of the favorable thermodynamics for EPT [see Eqs. (18)–(20)].[1,2,4,7,26,117–119,154,155] This reaction could also be described as $1e^-/1H^+$ MS-EPT. Electron transfer occurs from Tyr_Z to P_{680}^+ and simultaneous proton transfer from Tyr_Z-OH to His190, the latter through a preformed H-bond.

The $1e^-/1H^+$ MS-EPT pathway shown for Y_Z oxidation in Equations (18)–(20) is analogous to oxidation of ArOH in Equation (10) except that long-range (ca. 10 Å) electron transfer occurs from Tyr_Z to P_{680}^+ between fixed (nondiffusional) sites in the photosynthetic membrane.

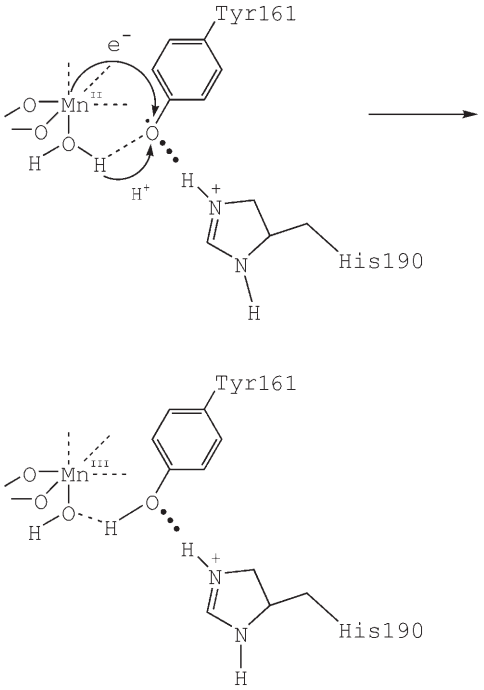

(22)

6.2. Oxidative Activation of the OEC

6.2.1. Introduction to Mechanism

As noted in the Introduction, several mechanistic models for water oxidation in the OEC have appeared over a period of years.[7,9,21,28,29,32,42–52] Stimulated by the recently published XRD and EXAFS structures of the OEC, our aim is to develop and apply a model for water oxidation, by building on the work of others, that is consistent with available experimental and theoretical results.

As with any mechanistic analysis of complex systems what is presented is a hypothesis. Although gross structural features of the OEC are available, key microscopic details (coordinated H_2O molecules, μ-oxido bridges, details of coordination environments) are not. The absence of these details necessarily creates ambiguities and uncertainties, which are highlighted in the discussion that follows. The conclusions reached should thus be taken with a "grain of salt".

6.2.2. The H-Abstraction Mechanism

In their analysis, Babcock and co-workers proposed that "H-abstraction" was also utilized in the oxidative activation of the OEC by $Y_Z^{\bullet}$.[1,2,4,7,26,27,39] As visualized for the $S_0 \rightarrow S_1$ transition in Equation (22), electron transfer was proposed to occur from Mn^{II} to Tyr-O$^{\bullet}$ accompanied by H^+ transfer from Mn–OH_2 to Tyr-O$^{\bullet}$.

This suggestion appears to be untenable given the structures in Figures 2–4, which reveal that Tyr_Z-OH is spatially separated from the nearest Mn ion in the {$CaMn_4$} cluster by around 6 Å. In view of the short-range nature of proton transfer in EPT, these distances would appear to rule out EPT as a viable pathway, and long-range EPT through a series of bridging H_2O molecules also seems unlikely.[90,93,98–100] There is some evidence that proton release may precede oxidation of Mn, perhaps induced by Y_Z (Tyr_Z-O–H···His190) oxidation/deprotonation;[156] however, careful inspection of the OEC structures in Figures 2–4 reveals other viable EPT pathways.

6.2.3. $1e^-/2H^+$ and Stepwise MS-EPT

MS-EPT pathways require prior H-bonding[157–162] because of the short-range nature of proton transfer. Possible MS-EPT pathways can be discerned in Figure 5 which utilize the putative Mn(4)–OH_2···Asp61 H-bond. Evidence for the importance of Asp61 is available from point-mutation studies on Asp61 in cells and oxygen-evolving core preparations from the wild type of *Synechocystis* sp. PCC 6803. Point mutation at Asp61 decreases the rate of oxygen release by a factor of 9–10. At the same time, the $S_1 \rightarrow S_2$ and $S_2 \rightarrow S_3$ transitions are slowed by a factor of 2–3, whereas reduction of P_{680}^+ by Y_Z is unaffected.[163]

$1e^-/2H^+$ MS-EPT: In the proposed MS-EPT pathway shown in Equation (23), the Mn(4)–OH_2···Asp61 H-bond participates in $1e^-/2H^+$ MS-EPT. In this pathway, electron transfer occurs from Mn(4) to $Tyr_Z^{\bullet}$ in concert with a double proton transfer. One proton transfers from Mn(4)–OH_2 to Asp61 and, simultaneously, the proton on $^+$H-His190 transfers to Tyr-O$^{\bullet}$.

There is no need to invoke a structural basis for interaction between transferring protons in Equation (23). Inherent in Equation (17) is the fact that EPT is a probabilistic consequence of the uncertainty principle in the same way as in electron transfer or proton transfer. EPT is induced by the electron-transfer matrix element and depends on the

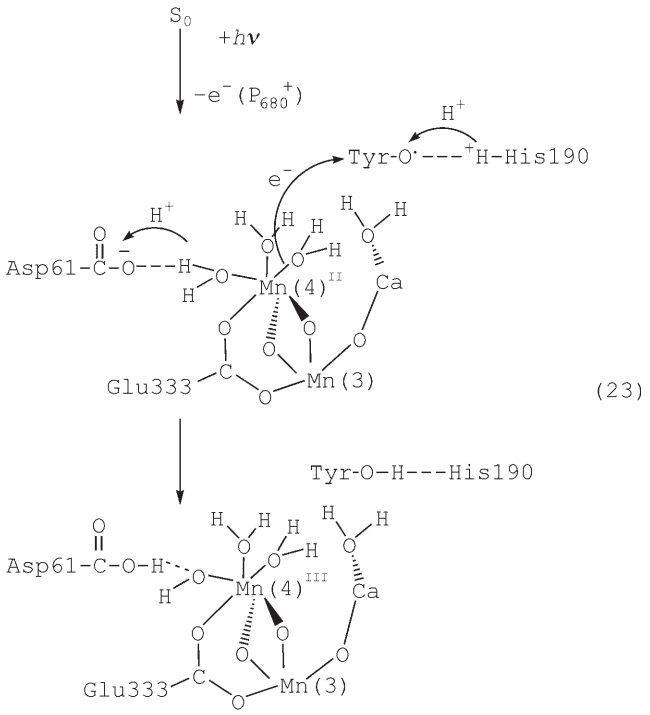

(23)

extent of vibrational overlap between the initial and final states for both transferring protons.

Stepwise 1 e⁻/1 H⁺ MS-EPT: MS-EPT oxidation of Mn(4) may also occur by stepwise $1e^-/1H^+$ MS-EPT with initial oxidation occurring at the Mn(3) center [Eq. (24)]. Oxidation at a cluster site or delocalized cluster orbital appears to occur in the $S_1 \rightarrow S_2$ transition (see Section 6.4).

In Equations (23) and (24), it is assumed that the S_0 oxidation-state distribution is $Mn^{II}Mn^{III}Mn^{IV}Mn^{IV}$. This assumption is commonly made[9,21,135,136,143,144] but, as noted in Section 5, appears to be inconsistent with the recent low-temperature EPR data of Kulik et al.[145] It is possible that the oxidation-state distribution in S_0 is temperature-dependent, and Mn^{II} is present at room temperature in the operating OEC.

In Equations (23) and (24), two couples undergo EPT: Tyr-O····⁺H-His190/Tyr-O–H···His190 ($Y_Z^{\bullet}/Y_Z$) and Mn^{III}-OH···HOOC-Asp61/Mn^{II}-OH_2···⁻OOC-Asp61. These couples act as "EPT modules" functioning together in $1e^-/2H^+$ MS-EPT to enable the simultaneous transfer of both electrons and protons.

For the Tyr_Z couple, the proton transferred from Tyr-OH to His190 in Equation (18) is transferred back in Equation (23) or (24). This "proton-rocking" mechanism was first proposed by Eckert and Renger[164] and has been elaborated by several groups since.[165–168] One important consequence of proton rocking is that it increases the oxidation potential of Tyr-O·. The increase of approximately 0.3 V relative to that of the Tyr-O·/Tyr-O⁻ couple is required for water oxidation to occur. Proton rocking also resets the Tyr-O–H···His190 interface for additional MS-EPT cycles (see Sections 6.5 and 6.6).

There is an energetic advantage for EPT over ET just as there is in the oxidation of Y_Z by P_{680}^+. Theoretical analysis gives a value of $\Delta G^\circ = +9.2\ kcal\,mol^{-1}$ for the electron transfer Mn^{II}-OH_2···Tyr-O·→Mn^{III}-OH_2^+···Tyr-O⁻.[39,154,155] The ET reaction is unfavorable because the initial products are formed in high-energy proton environments as can be surmised from the pK_a values ($pK_{a,1}([Mn^{III}(H_2O)_6]^{3+}) = 0.2$[169] and pK_a(Tyr-OH) = 10).[116]

6.3. Transitions between S States: $S_0 \rightarrow S_1$

Since S_1 is the stable resting state in the dark for the OEC, the dark-adapted, light-driven Kok cycle actually begins with the transition $S_1 \rightarrow S_2$. Oxygen is evolved following photoexcitation of S_3, and the fourth photoexcitation event converts S_0 into S_1. For purposes of mechanistic discussion, it is convenient to begin with the $S_0 \rightarrow S_1$ transition and follow the

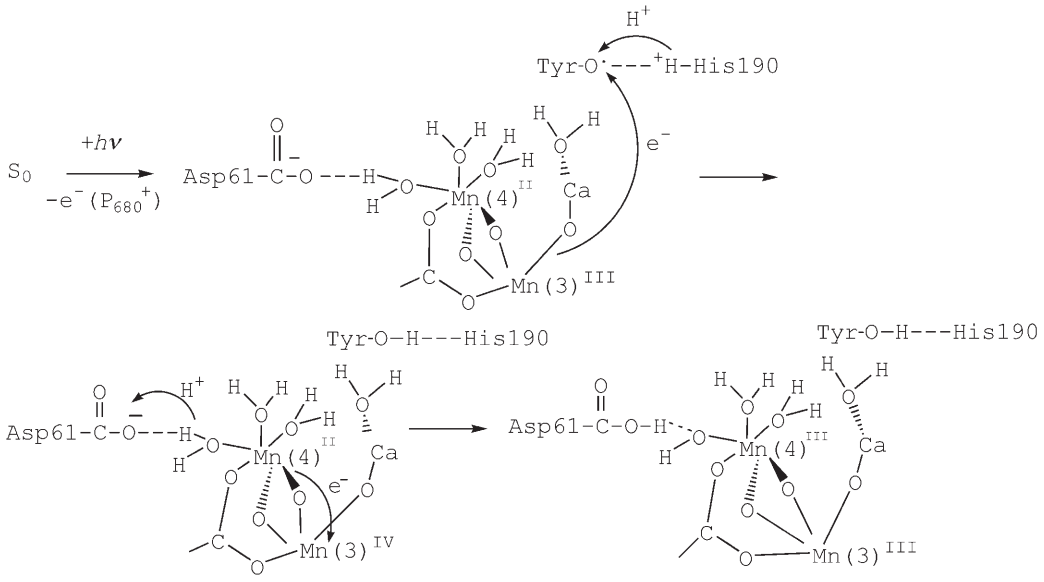

(24)

sequential buildup of redox equivalents as the cycle progresses.

On the basis of EXAFS measurements, the {$CaMn_4$} cluster has essentially the same structure in the S_1 and S_2 states. By contrast, there is an increase in one of the Mn···Mn distances by approximately 0.15 Å in S_0. This increase is consistent with protonation of a μ-oxido bridge or with the presence of one Mn^{II} center in S_0.[150,151]

6.3.1. MS-EPT Oxidation of the OEC

The $1e^-/2H^+$ and $1e^-/1H^+$ MS-EPT pathways in Equations (23) and (24) provide low-energy alternatives for oxidative activation of the OEC. The key structural elements are the Tyr-O•···$^+$H-His190 and Mn^{II}-OH_2···$^-$OOC-Asp61 hydrogen bonds, which enable EPT at each site. The MS-EPT pathway takes advantage of the relatively long-range nature of electron transfer[170,171] while meeting the short-range requirements of proton transfer.[58–68,70,90,93,98–100,172,173]

The active site for water oxidation appears to be Mn(4).[16,35] This conclusion is based on its proximity to the proton exit channel at Asp61 and its alignment toward the Ca^{2+} ion of the {$CaMn_3$} cluster, where O···O coupling appears to occur (see Section 6.5.2).

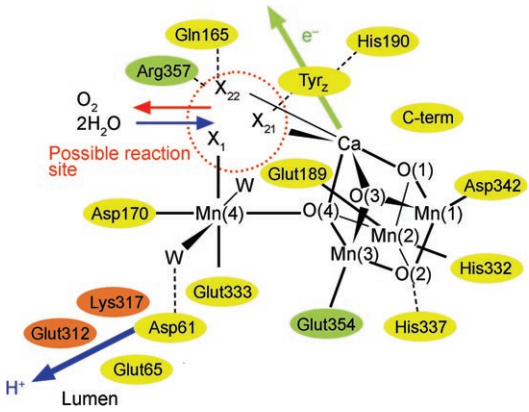

Figure 6. Schematic view of the OEC illustrating: 1) possible H-bond interactions between Tyr_Z and His190 and between $Mn(4)^{II}$–OH_2 (W = H_2O) and Asp61, shown as light blue dotted lines; 2) the hydrophilic exit channel for proton transfer from the entryway at Asp61 to the chloroplast lumen (large blue arrow); and 3) possible substrate water binding positions at Mn(4) (X_1) and Ca (X_{21} and X_{22}). Suggested O_2 exit and H_2O entry channels are shown by the red and blue arrows, respectively, and the direction of electron transfer to P_{680}^+ is shown by the green arrow. Residues in D1, D2, and CP43 subunits are shown in yellow, orange, and green, respectively. Another possible coordinated water molecule, not identified at 3.5-Å resolution, is shown as W. Reproduced from reference [16].

6.3.2. Long-Range H^+ Transfer to the Lumen

Following the loss of an electron in Equations (23) or (24), the first of four in the Kok cycle, a proton must be transferred to the chloroplast lumen. Proton transfer is required to avoid creating a local proton gradient, and it also resets the MS-EPT interface at Asp61.

Loss of protons to the exterior is facilitated by Asp61 as the EPT acceptor. As shown in Figure 6, Asp61 lies at the entryway to a hydrophilic proton exit channel to the lumen on the exterior of the PSII membrane. It is known that protons released in the Kok cycle appear on the lumen surface in as little as 12 μs.[163–165] The pK_a value of Asp61 is near the pH value of the lumen, which may be as low as pH 5.[165]

It has been proposed that a cluster of titratable residues participates in the proton exit channel beginning with Asp61 and terminating in a series of PsbO residues.[174–176] Relevant pK_a values and possible exit channels have been analyzed by solving the linearized Poisson–Boltzmann equation with atomic coordinates taken from the crystal structure at 3.0-Å resolution and CHARMM to optimize hydrogen-atom positions.[177] These calculations predict a monotonic increase in the pK_a value along the exit channel and identify an alternate channel from Asp61 to the lumen exit region in PsbO. They also identify a possible water-intake channel through a chain beginning at CP43-Arg357 and terminating at D_1His92 on the lumenal bulk surface.

In these calculations, charge was allowed to build up on the {$CaMn_4$} cluster rather than allowing for proton loss and redox-potential leveling. This results in greatly enhanced acidities for residues near the cluster, and these residues are suggested to be the origin of the released protons.[178]

The proton exit channel provides a mechanism for rapid proton loss to the lumen [Eq. (25)]. This step completes the loss of the first of four electrons and four protons required for water oxidation.

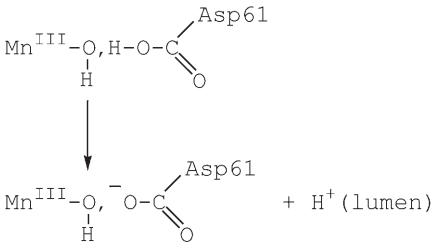

(25)

6.3.3. Intra-Coordination-Sphere H^+ Transfer

Following proton transfer to the lumen, Mn^{III}–OH remains at the interface with Asp61. A following step, in which intra-coordination-sphere proton transfer occurs [Eq. (26)], would have the advantage of re-forming the Mn(4)–OH_2–Asp61 interface, thus making it available for further $1e^-/2H^+$ MS-EPT cycles. Without this step, MS-EPT would produce inhibitory, high-energy Mn(4)–O^- intermediates.

Intra-coordination-sphere proton transfer has been demonstrated in metal complexes,[131,132,179] and there are elements that appear to promote it in the OEC. In Equation (26), the repulsive Mn–OH^-···$^-$OC(O)-Asp61 interaction is removed, and a stabilizing Mn^{III}–OH_2···Asp61 H-bond is formed. Transfer of OH^- to position X_1 in Figure 6 also appears to be favored by an electrostatic interaction with a positively charged side chain (-N(H)C$(NH_2)_2^+$) of CP43-Arg357$^+$.

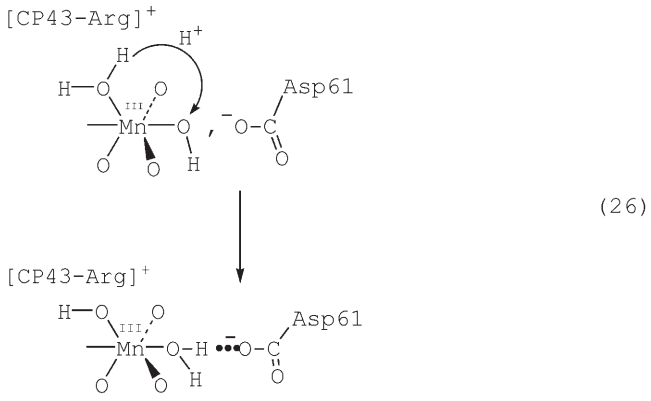

(26)

6.3.4. The Second Coordination Sphere: $^-$OOC-Asp170

The experimental pattern for proton release during the Kok cycle is 1:0:1:2[45,165,180–186] and not 1:1:1:1, although the latter pattern has been observed in spinach core particles.[187,188] The proton-release pattern is also pH-dependent.[185,189,190]

As discussed in Section 6.6, the final loss of two protons in a 1:0:1:2 pattern can be explained if it is assumed that aspartate Asp170 (shown coordinated to Mn(4) in Figures 2, 3, and 4, but at a distance of >3 Å in Figure 4) is actually in the second coordination sphere in the operating OEC as shown in Figures 4 and 5. Asp170 may act as an internal base toward deprotonation of Ca–OH_2 prior to O···O coupling (see Section 6.5.2).

Mutagenesis studies show that Asp170 is involved in the formation of the {Mn_4} cluster by providing a ligand at the high-affinity site that binds the first Mn ion.[191,192] It has been suggested on the basis of FTIR measurements on symmetric and asymmetric carboxylate modes of Asp170 that oxidation past S_0 does not involve Mn(4). Comparison of IR band shifts of the S state of wild-type PSII particles with those of the D1-Asp170His mutant PSII particles revealed no Asp170 IR band shifts upon oxidation of the OEC, although related cluster modes are known to respond to such changes.[21,124,146,193,194]

One explanation of the FTIR data, at least up to S_3, is that Mn(4) is not involved in the redox events at the OEC. Another explanation, consistent with the FTIR data and the structure in Figure 4, is that Asp170 is not coordinated to Mn(4) in the operating OEC.[194] With this interpretation, the second coordination sphere near the OEC includes anionic Asp170 ($^-$OOC-Asp170) rather than coordinated Asp170.

6.4. The $S_1 \rightarrow S_2$ Transition

The estimated increase in reduction potentials between the S_1/S_0 and S_2/S_1 couples is approximately 0.2 V,[122,123,195] which is small compared with differences between sequential couples for typical coordination complexes.[196,197] S_1 and S_2 are known from EXAFS measurements to have essentially the same structures.[150,152] There is general agreement that Mn^{III} oxidation to Mn^{IV} occurs in this transition, and, yet, there is evidence for Mn^{III} in EPR and NIR spectra from photolysis and spectroscopic measurements at -269 °C.[198]

The sequence in Equations (27) and (28), or stepwise MS-EPT as in Equation (24), could be invoked to explain the

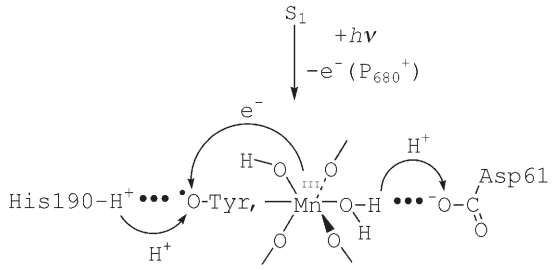

(27)

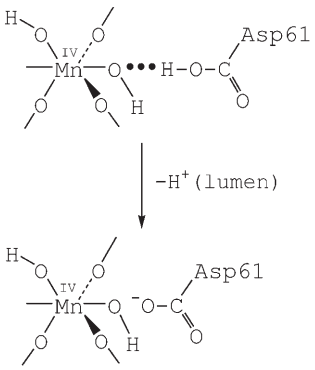

(28)

1:1:1:1 proton release pattern found in spinach core particles. However, the pattern in the operating OEC is 1:0:1:2. Also, there is evidence that Mn(4) is not oxidized in the $S_1 \rightarrow S_2$ transition.[138,140,199–201]

On the basis of resonant inelastic X-ray scattering (RIXS) measurements, it has been suggested that the electron lost in the $S_1 \rightarrow S_2$ transition comes from a delocalized orbital.[157,202] Shifts in IR band energies for $\nu(^-$OOC-) carboxylate modes from 1340 to 1430 cm^{-1} are observed in both the $S_1 \rightarrow S_2$ and $S_2 \rightarrow S_3$ transitions,[203–207] but significant shifts in α-$^-$OOC-D_1Alanine344 modes only occur in the $S_1 \rightarrow S_2$ and not in the $S_2 \rightarrow S_3$ transition.[207] Since D_1Ala344 is coordinated to Mn(2) (Figure 3), this result points to a contribution to the redox orbital from Mn(2) and, by inference, from the {$CaMn_3$} cluster in the $S_1 \rightarrow S_2$ transition. As noted above, FTIR data show that Asp170 is not affected.[21,124,193,194]

Oxidation to S_2 results in electrochromic band shifts, which have been interpreted as arising from a positive charge that is deeply buried away from bulk solvent in a low dielectric environment.[208,209] These electrochromic shifts only occur during the $S_1 \rightarrow S_2$ transition and are coupled with protein conformational changes.[21]

One explanation for these observations is that oxidation of S_1 occurs at the {$CaMn_3$} cluster, which creates an uncompensated positive charge and an increase in formal oxidation state of the cluster from $Mn_3^{III,IV,IV}$ to $Mn_3^{IV,IV,IV}$ [Eq. (29)]. In the absence of charge-compensating proton loss or addition of an anion, oxidation in the low-dielectric OEC membrane would create a positive charge, providing an explanation for the electrochromic effect.[27,210–212]

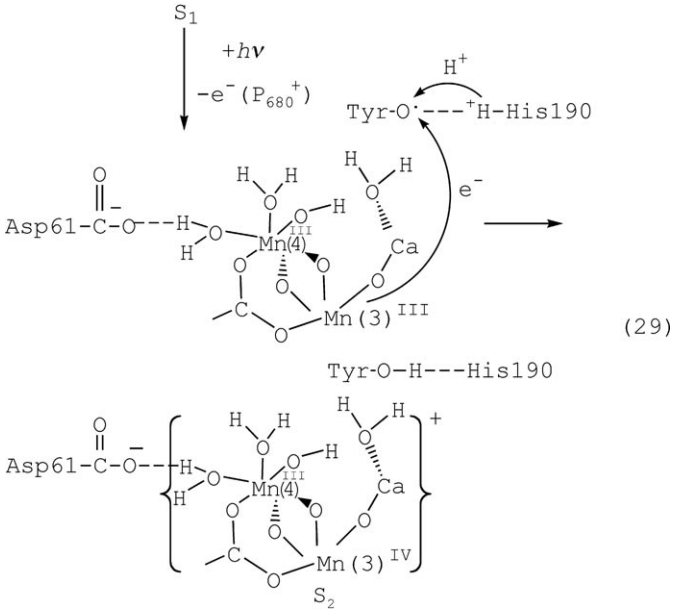

(29)

6.5. The $S_2 \rightarrow S_3 \rightarrow S_3'$ Transition

It has been suggested that O···O coupling occurs following oxidation of S_2 to S_3.[15,19,21,32,35,129,213] K-edge difference spectra from XANES measurements show that structural changes in the $S_1 \rightarrow S_2$ transition, which involve oxidation of Mn^{III} to Mn^{IV}, are significantly different from changes in the $S_2 \rightarrow S_3$ transition.[140,214] EXAFS data also point to a structural change between the S_2 and S_3 states,[20,42,49,203,215–218] but different results have been reported from different studies. An equilibrium between at least two states in S_3 has been proposed by Renger.[42,129] The energy of activation for the $S_2 \rightarrow S_3$ transition at 0.4 eV is the highest of the four S-state transitions.[126–128,219]

6.5.1. MS-EPT and PT in the $S_2 \rightarrow S_3$ Transition: The Intermediate State S_3

With the formulation of S_2 as in Equation (29), its further light-driven $1e^-/2H^+$ MS-EPT oxidation, with Asp61 as the proton acceptor, would give $Mn(4)^{IV}$ in its dihydroxido form $Mn^{IV}(OH)_2$ [Eq. (30)]. This suggestion is consistent with comparative XANES results on PSII and Mn model compounds, which suggest the absence of higher oxidation state Mn=O intermediates in all S states from S_0 to S_3.[220] There is evidence for Mn^{III} at this stage from liquid-helium EPR and NIR measurements, but note the discussion below.[156,198,221,222]

There is a debate in the literature as to whether oxidation at this stage is Mn-[49,135,138,170] or ligand-based.[136,140,144,223] Oxidation at a ligand, notably at a terminal or bridging oxido to give Mn(O•), is tantamount to saying that there is more ligand than metal character in the redox (HOMO) orbital.

With Mn-based oxidation and proton loss to the lumen as in Equation (30), a subsequent intra-coordination-sphere proton transfer [Eq. (31)] would reset the Mn(4)–OH_2···Asp61 MS-EPT interface. The local proton transfer channel shown in Equation (31) utilizes the putative third water molecule coordinated to Mn(4) shown in Figures 5 and 6. Intra-coordination-sphere proton transfer results in the intermediate labeled *S_3* in Equation (31). It is proposed to be the first of two forms of S_3 proposed by Renger.[42]

6.5.2. O···O Coupling: The $S_3 \rightarrow S_3'$ Transition

It is known that Ca depletion inhibits photosynthesis by blocking the $S_2 \rightarrow S_3$ transition, which implicates its participation in O···O coupling.[224–226] The coordination details around Ca in the OEC structures in Figures 2–6 are not established at 3- or 3.5-Å resolution. Nonetheless, as suggested in Figures 2 and 6, it is possible to place a water molecule coordinated to Ca in the position labeled X_{21} in Figure 6. On the basis of the relative positions of this putative Ca–OH_2 group and the

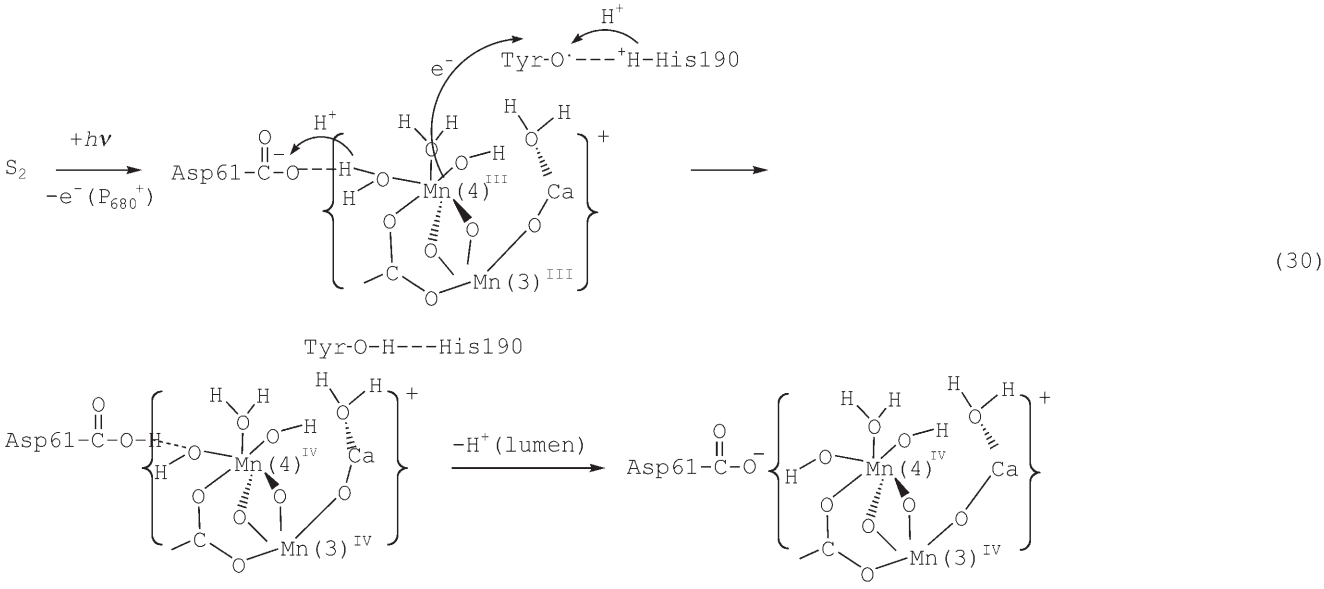

(30)

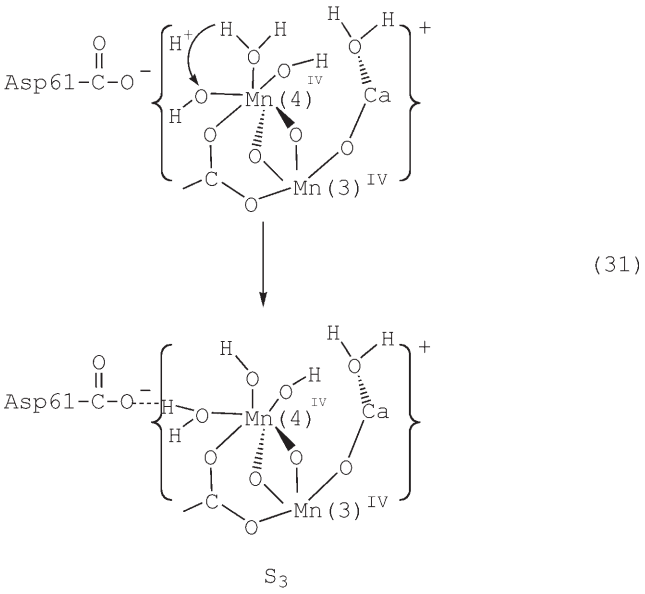

(31)

$Mn(4)^{IV}$–OH group at position X_1 in Figure 6, this has been proposed as the site for O···O coupling.[23,35]

The oxido form of $Mn(4)^{IV}$ (Mn^{IV}=O) is expected to be reactive toward O···O coupling.[25,26,32] It is available through the dihydroxido–oxido equilibrium, $Mn^{IV}(OH)_2 \rightleftharpoons Mn^{IV}(O)(H_2O)$, shown in Equation (32). There is precedence for related equilibria in metal complexes.[131–133]

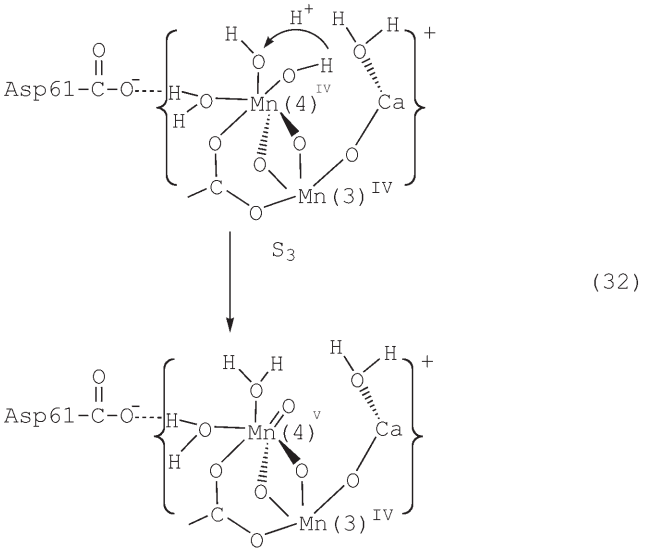

(32)

Even with access to Mn^{IV}=O, O···O coupling between Mn(4)=O and Ca–$OH_2(X_{22})$ without prior proton loss from the aqua ligand would give a high-energy, protonated peroxido intermediate $(H_2OO)Mn(H_2O)$. A more energetically reasonable proposal is that coupling is preceded by deprotonation to give Ca–$OH^-(X_{21})$,[32] but this would require an internal base. This is a role that may be played by Asp170, which is shown as occupying the second coordination sphere around Mn(4) in Figures 4 and 5. Equation (33) shows how Asp170 can act as an internal base toward proton loss from Ca–$OH_2(X_{21})$ by intervention of a local proton-transfer channel.

Other proton-transfer channels connecting Ca–OH_2 and $^-$OOC-Asp170 involving second-coordination-sphere water molecules, (not seen in the crystal structures) could be invoked which utilize a bridging H_2O molecule or molecules.[173] However, the use of H_2O as an acid (e.g., Mn(4)–OH···H–OH→$Mn(4)OH_2^+$···OH^-) or a base (e.g., Ca–OH_2···OH_2→Ca–OH^-···$^+HOH_2$) in a proton-transfer sequence is energetically unfavorable in view of the pK_a values $pK_a(H_2O) = 15.7$ and $pK_a(H_3O^+) = -1.74$.[157,202,203]

Proton loss from Ca–OH_2 and $Mn^{IV}(O)(H_2O)$ formation give intermediate **A**. It is proposed as the immediate precursor to O···O coupling. According to XANES and FTIR data, it is energetically unfavorable and does not build up as a detectable intermediate. Both the $Mn^{IV}(OH)_2 \rightleftharpoons Mn^{IV}(O)(H_2O)$ equilibrium and proton transfer in Equation (33) may be unfavorable. The latter is suggested by relative pK_a values for Ca^{2+}(aq) (9.7) and HOOC-Asp170 (4–5). The two preequilibria may contribute significantly to the high energy of activation (0.4 eV) for the $S_2 \rightarrow S_3$ transition.

The -$N(H)C(NH_2)_2^+$ guanidinium side chain of CP43-$Arg357^+$ spans the active face of the {$CaMn_3$} cluster and brackets the Ca–$OH_2(X_{21})$ coordination position. Mutagenesis studies show that CP43-$Arg357^+$ is required for O_2 evolution.[227] Its role may be through its electrostatic influence in decreasing the pK_a value for Ca–OH_2, which would decrease the difference in ΔG between intermediate **A** and S_3.

The proposed O···O coupling step in intermediate **A** is shown in Equation (34). In this reaction, Ca–OH^- redox nucleophilic attack on Mn=O occurs. Two electrons are transferred, either sequentially or in concert, one to $Mn(4)^{IV}$ and the other to the $Mn_3^{IV,IV,IV}$ cluster. The putative product of O···O coupling in Equation (34) is a Mn^{III}–hydroperoxide intermediate Mn^{III}–OOH. It is designated as S_3', the second of two proposed S_3 forms suggested by Renger.

Theoretical calculations have been carried out by Siegbahn and Crabtree on the O···O coupling step by assuming that Mn^V=O is the active intermediate.[28] Their calculations used density functional theory and the B3LYP functional for geometry optimization. The results of this calculation point to the importance of oxyl radical character ($Mn^{IV}(O^\bullet)$) in inducing O···O coupling.[25] They also suggest that Mn^{III}–OOH is in thermodynamic equilibrium with an activated Mn^V=O precursor. Similarly, Renger has proposed a rapid redox equilibrium between Mn-bound peroxide and two terminal hydroxido ligands.[42]

The proposal of two intermediates in S_3, defined here as S_3 and S_3', could provide an explanation for the conflicting EXAFS results if measurements were made on two different forms. In the interpretation of one EXAFS data set, the distances of 2.7 Å in the S_3 state lengthen to 2.8 and 3.0 Å, which is consistent with a reduced cluster and S_3'.[217] The interpretation of the second data set was consistent with Mn-centered oxidation of Mn^{III} to Mn^{IV} with associated structural changes. This observation would be consistent with S_3 before O···O coupling occurs.[214]

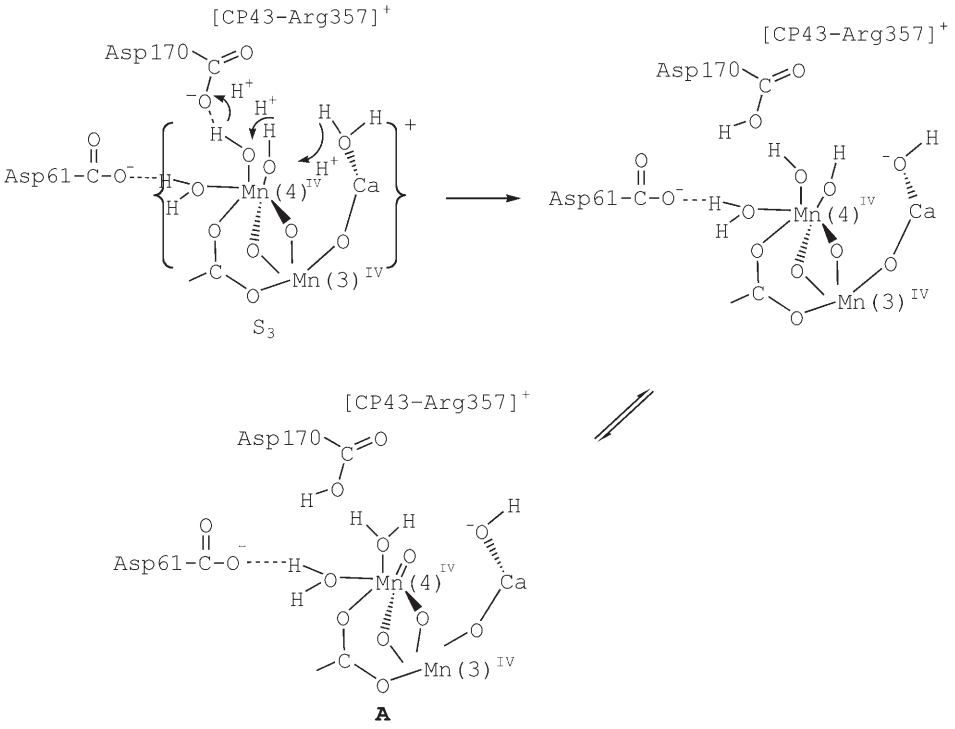

(33)

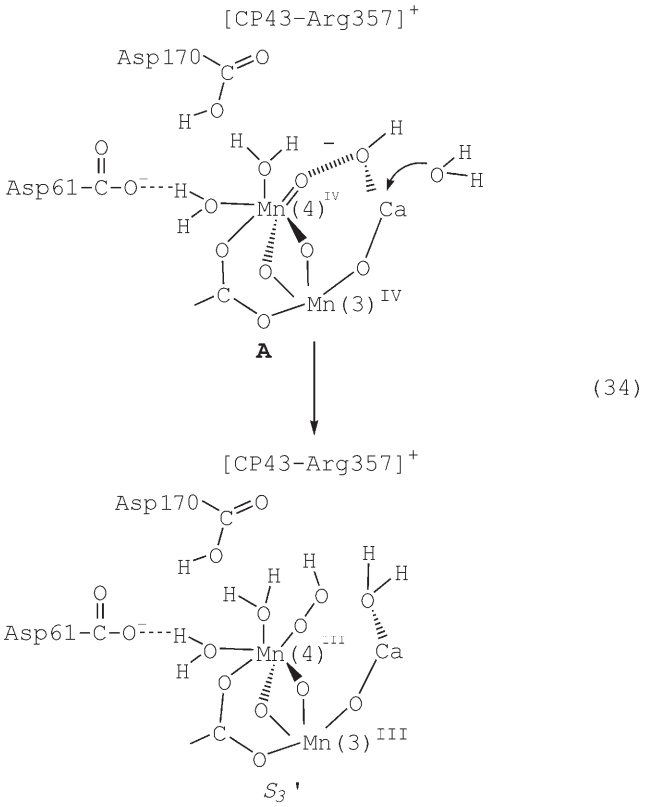

(34)

The results of water-exchange studies point to O···O coupling between different sites, one of which undergoes rapid exchange with external solvent and the other undergoes slow exchange.[21,48,228–231] The rapidly exchanging site is presumably Ca–OH_2, and exchange either occurs in S_3 before O···O coupling or occurs after coupling if there is a rapid equilibrium between S_3 and S_3'.

The site for slow exchange is presumably Mn(4). A likely mechanism for solvent exchange at Mn would involve the $Mn^{IV}(OH)_2 \rightleftharpoons Mn^{IV}(O)(H_2O)$ equilibrium in Equation (32) with net exchange occurring by the sequence: 1) HO–Mn–O*H → O=Mn–O*H_2 (oxido–dihydroxido equilibration), 2) O=Mn–O*$H_2 + H_2O \rightarrow$ O=Mn–$OH_2 + H_2O$* (water exchange), 3) O=Mn–$OH_2 \rightarrow$ HO–Mn–OH.[131,132,179]

Cl^- was not located in the 3.5-Å-resolution structure, but it is a cofactor for water oxidation, even though chloride-depleted samples can be reconstituted to catalytically active forms by addition of a variety of anions.[232–234] The results of a recent combined EPR–FTIR study are consistent with N_3^- binding in the immediate vicinity of the Mn cluster and show that Cl^- binding is competitive with N_3^- binding at this site.[235]

McEvoy and Brudvig[35] suggested that activation by Cl^- binding to Mn(4) could occur by coordination expansion or Cl^- bridging between Ca and Mn(4). In either case, a coordinated anion could play an indirect role through its electronic influence on pK_a values and intermolecular proton transfer. For example, anion transfer from Ca to Mn(4) would enhance Ca–OH_2 acidity and favor proton transfer from Ca–OH_2 to $^-$OOC-Asp170 in Equation (33).

The role of spin exchange in electron transfer and O···O coupling remains to be evaluated. The EPR spectrum of S_3 was first reported by Matsukawa, et al., who also reported a phenomenological simulation.[236]

6.6. $S_3 \rightarrow S_4 \rightarrow S_0 + O_2$: O_2 Evolution

States S_0, S_1, S_2, and S_3 have all been trapped and investigated spectroscopically. Photoexcitation of S_3 results in O_2 evolution and simultaneous appearance of S_0. The

reduction of $Y_Z^{\bullet}$ is rate-limiting. Evidence for a transient S_4 state from transient EPR measurements has been reported.[237] Recently, inhibition of O_2 evolution from cyanobacteria was observed at high O_2 pressures with associated UV spectral changes that provided additional evidence for an intermediate past the S_3 state.[51,238] Even more recently, time-resolved X-ray absorption spectroscopy (XAS) measurements have provided direct evidence for an intermediate following photoexcitation of S_3.[215] Following laser flash photolysis, oxidation of Mn by electron transfer to $Y_Z^{\bullet}$ occurs on a timescale of 1.1 ms, which is somewhat dependent on the sample type.[163] In the transient XAS experiment, reduction at Mn is preceded by a lag phase of 250 μs. This transient event is entropically driven, does not involve Mn=O, and does not affect the oxidation states of either Mn or $Y_Z^{\bullet}$.

It has been concluded that the lag phase is most likely due to a proton-transfer step.[215] A proposal that a proton transfer preceded electron transfer was originally made by Rappaport et al.[209] The kinetics of $Y_z^{\bullet}$ reduction by the OEC and of O_2 release, following excitation of S_3, are known to be very similar, and both occur on the millisecond timescale.[237]

In view of the absence of detailed experimental information, any mechanistic interpretation of the $S_3 \rightarrow [S_4] \rightarrow S_o + O_2$ transition is necessarily speculative. Nonetheless, it is possible to account for a lag phase and, ultimately, for O_2 evolution on the basis of a series of reactions that utilize EPT and stepwise PT. The mechanism below is only suggestive but it does present a reasonable account of the final steps that may occur leading to O_2 evolution.

The initial step in this mechanism is the light-driven, $1e^-/1H^+$ MS-EPT oxidation of Y_Z, as shown in Equation (35). Following this initial redox step, internal proton transfer is shown from bound peroxide to Asp61. This step is proposed to be the origin of the 250-μs lag phase in the XAS measurements.

Loss of the peroxidic proton would activate coordinated peroxide toward electron transfer to $Y_Z^{\bullet}$. This reaction is also shown in Equation (35), but it may occur stepwise with initial oxidation at Mn(4) ($Mn^{III}(OO^{2-}),Y_Z^{\bullet} \rightarrow Mn^{IV}(OO^{2-}),Y_Z$), followed by intramolecular electron transfer ($Mn^{IV}(OO^{2-}),Y_Z \rightarrow Mn^{III}(OO^{-\bullet}),Y_Z$). From the experimental results, all steps subsequent to electron transfer are rapid on a timescale of around 1 ms.

In the final step in Equation (35), a proton is lost from Asp61 to the lumen. This would open up a stepwise, long-range proton-transfer channel from HOOC-Asp170 to Asp61 [Eq. (36)]. Subsequent loss of this second proton to the lumen would provide an explanation for the 1:0:1:2 proton-release pattern and loss of two protons in the $S_3 \rightarrow \{S_4\} \rightarrow S_0 + O_2$ transition.

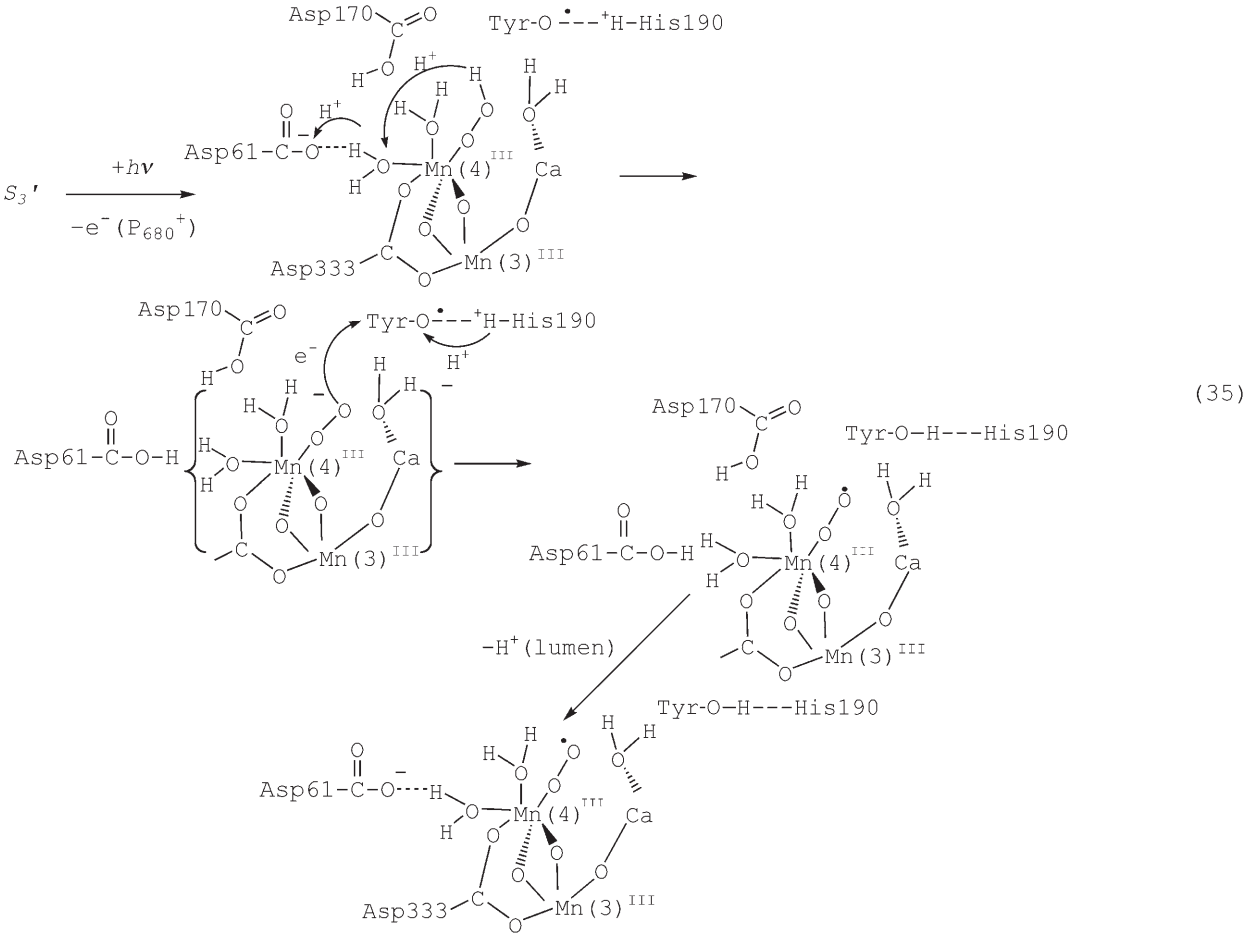

(35)

Also, as shown in Equation (36), subsequent intra-coordination-sphere proton transfer would reset Mn(4)–OH_2 at the Asp61 interface. The final product of the series of reactions proposed in Equations (35) and (36) is a superoxide complex of Mn^{III}, $Mn^{III}(OO^{-\bullet})$. It is tentatively identified as S_4 and is presumably the intermediate that was observed at high added partial pressures of O_2 by Clausen and Junge, which they formulated as an intermediate peroxide.[238]

The net reaction in the sequence in Equations (35) and (36) is electron transfer from coordinated $^{-}$OOH to $Y_Z^{\bullet}$ coupled with proton transfer to the lumen ($Y_Z^{\bullet}$,Mn^{III}–OOH → Y_Z,Mn^{III}–$O_2^{\bullet}$ + H^+(lumen). There is no change in oxidation state at Mn and the rate-limiting step is intra-coordination-sphere proton transfer.

In the final step of our proposed catalytic cycle, intramolecular electron transfer occurs from O_2^- to the $Mn(4)^{III}$. This is followed by loss of O_2 and coordination of H_2O to return the catalytic system to S_0. This reaction is shown as reversible in Equation (37), which is consistent with the high-pressure results of Clausen and Junge.[238]

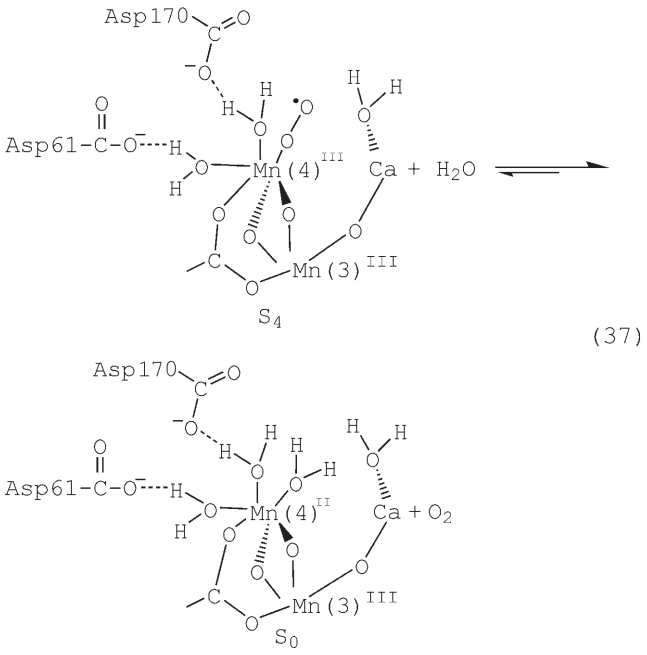

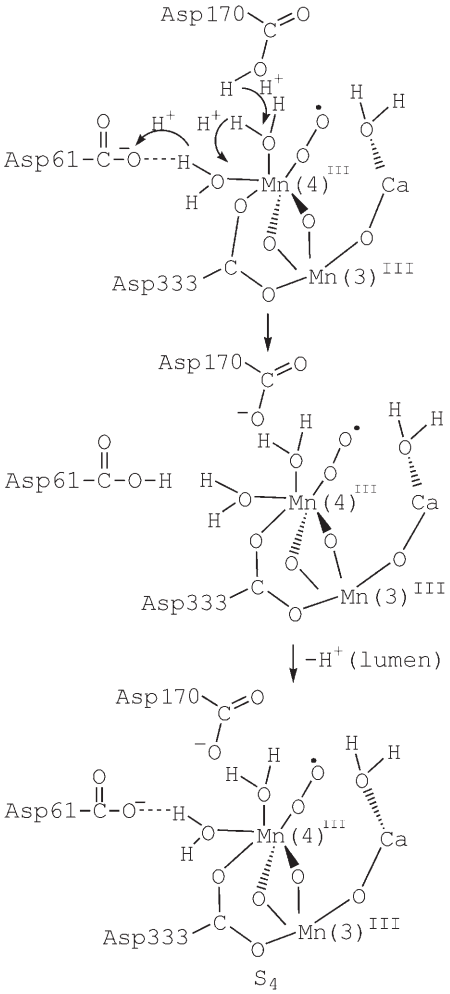

7. Reaction Summary

The proposed reactions and intermediates as well as the identities of the S states in the Kok cycle are all summarized in Scheme 1. The perspectives, orientation, and positions of key groups are based on the EXAFS structure in Figure 4. The summary is based on analyses of individual S-state transitions in the text. In some cases, there are ambiguities in detail and the discussion in the individual sections should be consulted. The summary is based on the following assumptions:

1) Asp170 is uncoordinated in all S states.
2) Oxidation in the $S_1 \rightarrow S_2$ transition occurs at the {$CaMn_3$} cluster, which increases its formal oxidation state from $Mn_3^{III,IV,IV}$ to $Mn_3^{IV,IV,IV}$ and creates a local positive charge.
3) Oxidation in the $S_2 \rightarrow S_3$ transition occurs at Mn(3) to give $Mn^{IV}(OH)_2$, the first of two intermediates in S_3. The first intermediate, S_3, precedes O···O coupling; the second, S_3', is the putative coupling product $Mn(4)^{III}$–OOH.
4) $^{-}$OOC-Asp170 acts as an internal base for deprotonation prior to electron transfer in the $S_2 \rightarrow S_3$ transition. Release of the Asp170 proton in the transition $S_3 \rightarrow [S_4] \rightarrow S_0 + O_2$ provides a second proton, explaining the 1:0:1:2 proton-release pattern.
5) In the transition $S_3 \rightarrow [S_4] \rightarrow S_0 + O_2$, rate-limiting deprotonation of $Mn(4)^{III}$–OOH is followed by oxidation by $Y_Z^{\bullet}$ to give S_4. S_4 is assumed to be Mn^{III}–$OO^{\bullet}$, an Mn^{III} superoxide complex that forms reversibly from S_0 at high partial pressures of O_2.

8. Summary and Outlook

Notable features in this analysis of proton-coupled electron transfer (PCET) in photosystem II (PSII) are the

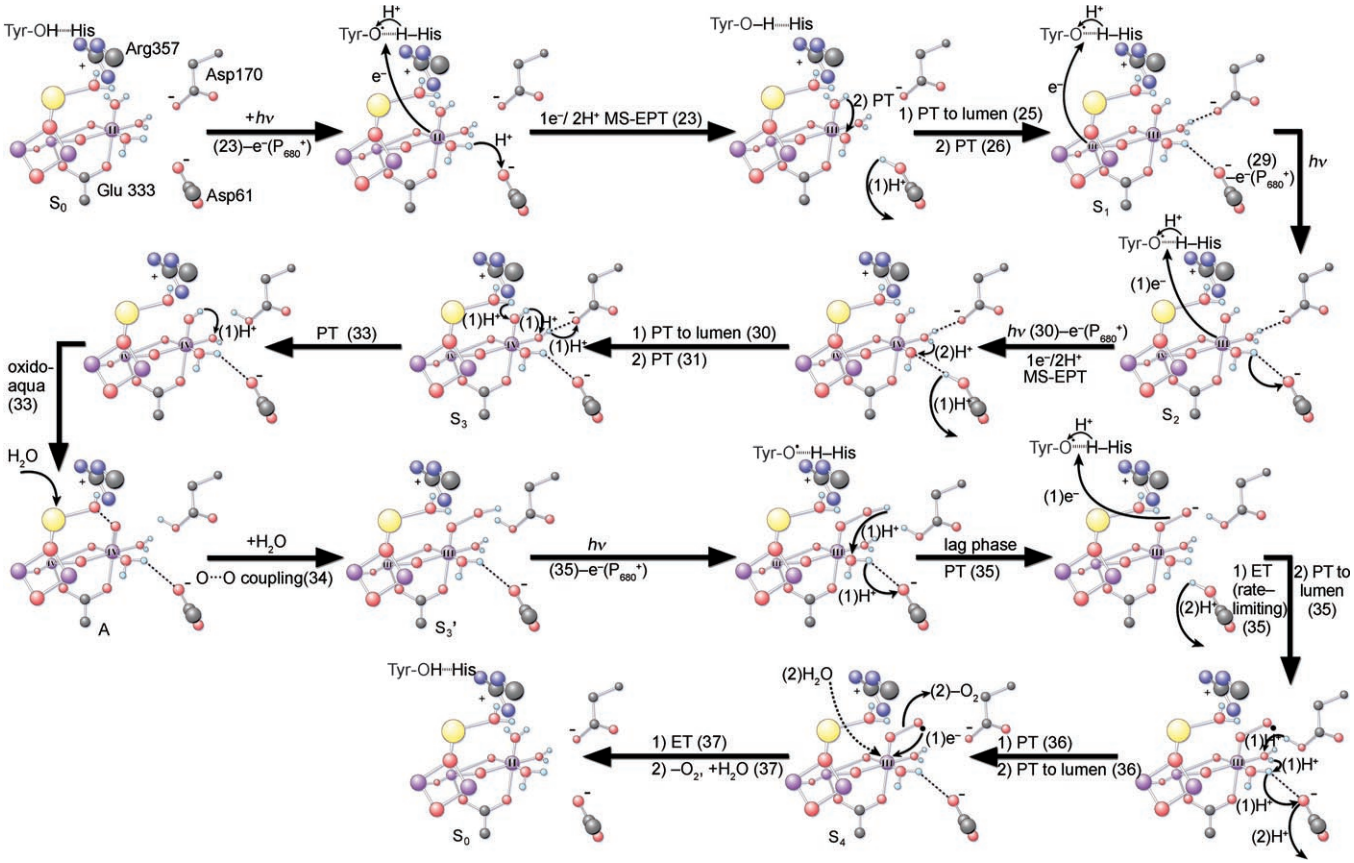

Scheme 1. Summary of the reactions. The Ca center in the {$CaMn_3$} cluster is yellow, Mn purple, O red, N blue, C blue. As a guide, the numbers in parentheses indicate the corresponding equations in the text. The relevant oxidation states of Manganese are given in Roman numerals.

critical roles played by proton transfer (PT) and coupled electron–proton transfer (EPT). These appear to be essential elements in water oxidation by the oxygen-evolving complex (OEC). The structural focus on proton transfer is a direct consequence of its short-range nature relative to electron transfer. In the PSII structure, electron transfer appears to be a relative afterthought; the demands of short-range proton transfer dominate, which leads to the concept of "proton wiring". Local proton-transfer channels, consisting of sequences of short-range, stepwise proton transfers, are a critical element in the OEC. They allow released protons to be delivered over long distances to a proton exit channel. They also allow the activation of key functional groups toward O···O coupling and electron transfer.

A key element in achieving local proton equilibration is intra-coordination-sphere proton transfer between H_2O and OH^- ligands at the Mn(4) center, the non-{$CaMn_3$} cluster site in the OEC where O···O coupling appears to occur. These transfers orient an oxido group at the Mn(4) center for O···O coupling. They also maintain Mn(4)–OH_2 at an interface with Asp61, the entryway to the proton exit channel to the lumen. A second key element is Asp170. Although apparently not coordinated, it may act as an internal base for deprotonation of Ca–OH_2 prior to O···O coupling and intramolecular electron transfer.

EPT provides a pathway for light-driven oxidation of the OEC at each stage of the Kok cycle. The key is the use of a series of multiple site-EPT (MS-EPT) pathways in which electron transfer is coupled to proton transfer. These pathways exploit the long-range nature of electron transfer while meeting the structural needs of short-range proton transfer. EPT pathways lower reaction barriers by avoiding high-energy intermediates that arise from initial electron transfer or proton transfer.

The mechanism of water oxidation at the OEC is complicated, which is a natural consequence of its multielectron, multiproton character. In its use of EPT and local and long-range proton transfer, it shares features with other biological PCET reactions.[68,239,240] The pathways exploited by the OEC are general and used in other biological PCET reactions as well.

The mechanistic details proposed herein are largely consistent with available experimental data. As in any chemical mechanism, the explicit details remain open to further experimental and theoretical elucidation. Hopefully, our efforts will provide a useful framework for probing even more deeply into water oxidation in the OEC.

Authors would like to acknowledge Ms. Aimee Worden for help with the illustrations, Warwick Hillier of ANU, Canberra,

for helpful discussions and for providing a preprint of reference [21], and the US National Science Foundation and the US Department of Energy for financial support.

Received: March 9, 2006
Revised: December 19, 2006

[1] C. Tommos, G. T. Babcock, *Acc. Chem. Res.* **1998**, *31*, 18 – 25.
[2] C. W. Hoganson, G. T. Babcock, *Science* **1997**, *277*, 1953 – 1956.
[3] A. Remy, K. Gerwert, *Nat. Struct. Biol.* **2003**, *10*, 637 – 644.
[4] G. T. Babcock, M. Espe, C. Hoganson, N. Lydakis-Simantiris, J. McCracken, W. J. Shi, S. Styring, C. Tommos, K. Warncke, *Acta Chem. Scand.* **1997**, *51*, 533 – 540.
[5] D. A. Proshlyakov, M. A. Pressler, G. T. Babcock, *Proc. Natl. Acad. Sci. USA* **1998**, *95*, 8020 – 8025, and references therein.
[6] J. Barber, *Q. Rev. Biophys.* **2003**, *36*, 71 – 89.
[7] B. A. Diner, G. T. Babcock, *Advances in Photosynthesis: The Light Reactions*, *Vol. 4* (Eds.: D. R. Ort, C. F. Yocum), Kluwer Academic, Dordrecht, **1996**, pp. 213 – 247.
[8] B. A. Diner, F. Rappaport, *Annu. Rev. Plant Biol.* **2002**, *53*, 551 – 580.
[9] V. K. Yachandra, K. Sauer, M. P. Klein, *Chem. Rev.* **1996**, *96*, 2927 – 2950.
[10] W. Ruttinger, G. C. Dismukes, *Chem. Rev.* **1997**, *97*, 1 – 24.
[11] R. D. Britt, D. R. Ort, C. F. Yocum in *Advances in Photosynthesis*, *Vol. 4*, Kluwer Academic, **1996**, pp. 137.
[12] J. Barber, *Biochim. Biophys. Acta* **1998**, *1365*, 269 – 277.
[13] J. E. Penner-Hahn, *Met. Sites Proteins Models* **1998**, *90*, 1 – 36.
[14] J. H. A. Nugent, *Biochim. Biophys. Acta* **2001**, *1503*, 288 – 298.
[15] B. Ke in *Photosynthesis-Photobiochemistry and Photobiophysics*, Kluwer Academic, Dordrecht, **2001**.
[16] K. N. Ferreira, T. M. Iverson, K. Maghlaoui, J. Barber, S. Iwata, *Science* **2004**, *303*, 1831 – 1838.
[17] A. Zouni, H. T. Witt, J. Kern, P. Fromme, N. Krauss, W. Saenger, P. Orth, *Nature* **2001**, *409*, 739 – 743.
[18] N. Kamiya, J. R. Shen, *Proc. Natl. Acad. Sci. USA* **2003**, *100*, 98 – 103.
[19] C. Goussias, A. Boussac, A. W. Rutherford, *Philos. Trans. R. Soc. London Ser. B* **2002**, *357*, 1369 – 1381.
[20] K. Sauer, V. K. Yachandra, *Biochim. Biophys. Acta* **2004**, *1655*, 140 – 148.
[21] "Photosystem II: The Water/Plastoquinone Oxido-Reductase of Photosynthesis": W. Hillier, J. Messinger, V. K. Yachandra in *The Catalytic Manganese Cluster* (Eds.: T. Wydrzynski, K. Satoh) Kluwer Academic, Dordrecht, **2005**, pp. 567 – 608.
[22] J. Biesiadka, B. Loll, J. Kern, K.-D. Irrgang, A. Zouni, *Phys. Chem. Chem. Phys.* **2004**, *6*, 4733 – 4736.
[23] B. Loll, J. Kern, W. Saenger, A. Zouni, J. Biesiadka, *Nature* **2005**, *438*, 1040 – 1044.
[24] B. Kok, B. Forbush, M. McGloin, *Photochem. Photobiol.* **1970**, *11*, 457 – 475.
[25] F. Himo, P. E. M. Siegbahn, *Chem. Rev.* **2003**, *103*, 2421 – 2456.
[26] G. T. Babcock, M. Wikström, *Nature* **1992**, *356*, 301 – 309.
[27] C. Tommos, C. W. Hoganson, M. Di Valentin, N. Lydakis-Simantiris, P. Dorlet, K. Westphal, H. A. Chu, J. McCracken, G. T. Babcock, *Curr. Opin. Chem. Biol.* **1998**, *2*, 244 – 252.
[28] P. E. M. Siegbahn, R. H. Crabtree, *J. Am. Chem. Soc.* **1999**, *121*, 117 – 127.
[29] J. S. Vrettos, J. Limburg, G. W. Brudvig, *Biochim. Biophys. Acta* **2001**, *1503*, 229 – 245.
[30] M. Haumann, W. Junge, *Biochim. Biophys. Acta* **1999**, *1411*, 86 – 91.
[31] J. H. A. Nugent, R. J. Ball, M. C. W. Evans, *Biochim. Biophys. Acta* **2004**, *1655*, 217 – 221.
[32] V. L. Pecoraro, M. J. Baldwin, M. T. Caudle, W. Y. Hsieh, N. A. Law, *Pure Appl. Chem.* **1998**, *70*, 925 – 929.
[33] A. Ehrenberg, *Biochim. Biophys. Acta* **2004**, *1655*, 231 – 234.
[34] P. E. M. Siegbahn, *Curr. Opin. Chem. Biol.* **2002**, *6*, 227 – 235.
[35] J. P. McEvoy, G. W. Brudvig, *Phys. Chem. Chem. Phys.* **2004**, *6*, 4754 – 4763.
[36] H. T. Witt, *Ber. Bunsen-Ges.* **1996**, *100*, 1923 – 1942.
[37] R. J. Debus, *Biochim. Biophys. Acta* **1992**, *1102*, 269 – 352.
[38] M. L. Gilchrist, J. A. Ball, D. W. Randall, R. D. Britt, *Proc. Natl. Acad. Sci. USA* **1995**, *92*, 9545 – 9549.
[39] C. W. Hoganson, N. Lydakis-Simantiris, X. S. Tang, C. Tommos, K. Warncke, G. T. Babcock, B. A. Diner, J. McCracken, S. Styring, *Photosynth. Res.* **1995**, *46*, 177 – 184.
[40] H. H. Thorp, J. E. Sarneske, G. W. Brudig, R. H. Crabtree, *J. Am. Chem. Soc.* **1989**, *111*, 9249 – 9250.
[41] M. J. Baldwin, N. A. Law, T. L. Stemmler, J. W. Kampf, J. E. Penner-Hahn, V. L. Pecoraro, *Inorg. Chem.* **1999**, *38*, 4801 – 4809.
[42] G. Renger, *Biochim. Biophys. Acta* **2004**, *1655*, 195 – 204.
[43] G. W. Brudvig, R. H. Crabtree, *Proc. Natl. Acad. Sci. USA* **1986**, *83*, 4586 – 4588.
[44] A. G. Volkov, *Bioelectrochem. Bioenerg.* **1989**, *21*, 3 – 24.
[45] E. Schlodder, H. T. Witt, *J. Biol. Chem.* **1999**, *274*, 30387 – 30392.
[46] G. Renger, *Mech. Physiol. Plant* **1997**, *100*, 828 – 841.
[47] J. Dasgupta, R. T. van Willigen, G. C. Dismukes, *Phys. Chem. Chem. Phys.* **2004**, *6*, 4793 – 4802.
[48] J. Messinger, M. Badger, T. Wydrzynski, *Proc. Natl. Acad. Sci. USA* **1995**, *92*, 3209 – 3213.
[49] H. Dau, L. Iuzzolino, J. Dittmer, *Biochim. Biophys. Acta* **2001**, *1503*, 24 – 39.
[50] J. Limburg, J. S. Vrettos, L. M. Liable-Sands, A. L. Rheingold, R. H. Crabtree, G. W. Brudvig, *Science* **1999**, *283*, 1524 – 1527.
[51] J. Messinger, *Phys. Chem. Chem. Phys.* **2004**, *6*, 4764 – 4771.
[52] P. E. M. Siegbahn, *Inorg. Chem.* **2000**, *39*, 2923 – 2935.
[53] R. A. Binstead, B. A. Moyer, G. J. Samuels, T. J. Meyer, *J. Am. Chem. Soc.* **1981**, *103*, 2897 – 2899.
[54] R. A. Binstead, M. E. McGuire, A. Dovletoglou, W. K. Seok, L. E. Roecker, T. J. Meyer, *J. Am. Chem. Soc.* **1992**, *114*, 173 – 186.
[55] J. P. Roth, S. Lovell, J. M. Mayer, *J. Am. Chem. Soc.* **2000**, *122*, 5486 – 5498.
[56] N. Iordanova, H. Decornez, S. Hammes-Schiffer, *J. Am. Chem. Soc.* **2001**, *123*, 3723 – 3733.
[57] J. M. Mayer, D. A. Hrovat, J. L. Thomas, W. T. Borden, *J. Am. Chem. Soc.* **2002**, *124*, 11142 – 11147.
[58] D. Borgis, J. T. Hynes, *J. Phys. Chem.* **1996**, *100*, 1118 – 1128.
[59] R. I. Cukier, J. Zhu, *J. Phys. Chem. B* **1997**, *101*, 7180 – 7190.
[60] R. P. Bell, *The Tunnel Effect in Chemistry*, Chapman and Hall, London, **1980**.
[61] D. Borgis, J. T. Hynes, *Chem. Phys.* **1993**, *170*, 315 – 346.
[62] S. G. Christov, *Chem. Phys.* **1992**, *168*, 327 – 329.
[63] A. Warshel, *Acc. Chem. Res.* **2002**, *35*, 385 – 395.
[64] L. I. Krishtalik, *Biochim. Biophys. Acta* **2000**, *1458*, 6 – 27.
[65] J. T. Hynes, *Nature* **1999**, *397*, 565 – 567.
[66] K. Ando, J. T. Hynes, *J. Phys. Chem. B* **1997**, *101*, 10464 – 10478.
[67] K. Ando, J. T. Hynes, *J. Phys. Chem. A* **1999**, *103*, 10398 – 10408.
[68] P. L. Geissler, C. Dellago, D. Chandler, J. Hutter, M. Parrinello, *Science* **2001**, *291*, 2121 – 2124.
[69] J. M. Mayer, *Acc. Chem. Res.* **1998**, *31*, 441 – 450.
[70] K. Ando, J. T. Hynes, *Adv. Chem. Phys.* **1999**, *110*, 381 – 430.
[71] K. A. Gardner, L. L. Kuehnert, J. M. Mayer, *Inorg. Chem.* **1997**, *36*, 2069 – 2078.
[72] L. R. Mahoney, M. A. Darooge, *J. Am. Chem. Soc.* **1975**, *97*, 4722 – 4731.
[73] K. U. Ingold, G. A. Russell in *Free Radicals* (Ed.: J. K. Kochi), Interscience, New York, **1973**, pp. 275.

[74] Landolt-Börnstein, *Radical Reaction Rates in Liquids*, New Series, Vol. II/13, Springer, New York, **1984**; Landolt-Börnstein, *Radical Reaction Rates in Liquids*, New Series, Vol. II/18, Springer, New York, **1994**.
[75] J. M. Tedder, *Angew. Chem.* **1982**, *94*, 433 – 442; *Angew. Chem. Int. Ed. Engl.* **1982**, *21*, 401 – 410.
[76] J. M. Mayer, *Biomimetic Oxidations Catalyzed by Transition Metal Complexes* (Ed.: B. Meunier), Imperial College Press, London, **2000**, pp. 1 – 43.
[77] K. Wang, L. L. Kuehnert, J. M. Mayer, *J. Org. Chem.* **1997**, *62*, 4248 – 4252.
[78] L. Roecker, T. J. Meyer, *J. Am. Chem. Soc.* **1986**, *108*, 4066 – 4073.
[79] K. A. Gardner, J. M. Mayer, *Science* **1995**, *269*, 1849 – 1851.
[80] P. K. Agarwal, S. P. Webb, S. Hammes-Schiffer, *J. Am. Chem. Soc.* **2000**, *122*, 4803 – 4812.
[81] J. P. Klinman, *Crit. Rev. Biochem.* **1981**, *10*, 39 – 78.
[82] G. Pettersson, *Crit. Rev. Biochem. Mol. Biol.* **1987**, *21*, 349 – 389.
[83] M. H. V. Huynh, T. J. Meyer, *Chem. Rev.* **2007**, submitted.
[84] L. Biczok, N. Gupta, H. Linschitz, *J. Am. Chem. Soc.* **1997**, *119*, 12601 – 12609.
[85] L. Biczok, H. Linschitz, *J. Phys. Chem.* **1995**, *99*, 1843 – 1845.
[86] D. Shukla, R. H. Young, S. Farid, *J. Phys. Chem. A* **2004**, *108*, 10386 – 10394.
[87] R. I. Cukier, *J. Phys. Chem.* **1995**, *99*, 16101 – 16115.
[88] R. I. Cukier, *J. Phys. Chem.* **1994**, *98*, 2377 – 2381.
[89] X. G. Zhao, R. I. Cukier, *J. Phys. Chem.* **1995**, *99*, 945 – 954.
[90] R. I. Cukier, D. G. Nocera, *Annu. Rev. Phys. Chem.* **1998**, *49*, 337 – 369.
[91] R. I. Cukier, *J. Phys. Chem.* **1996**, *100*, 15428 – 15443.
[92] R. I. Cukier, *J. Phys. Chem. B* **2002**, *106*, 1746 – 1757.
[93] R. I. Cukier, *Biochim. Biophys. Acta* **2004**, *1655*, 37 – 44.
[94] H. Decornez, S. Hammes-Schiffer, *J. Phys. Chem. A* **2000**, *104*, 9370 – 9384.
[95] J.-Y. Fang, S. Hammes-Schiffer, *J. Chem. Phys.* **1997**, *107*, 5727 – 5739.
[96] J.-Y. Fang, S. Hammes-Schiffer, *J. Chem. Phys.* **1997**, *107*, 8933 – 8939.
[97] J.-Y. Fang, S. Hammes-Schiffer, *J. Chem. Phys.* **1997**, *106*, 8442 – 8454.
[98] S. Hammes-Schiffer, *Acc. Chem. Res.* **2001**, *34*, 273 – 281.
[99] S. Hammes-Schiffer, *ChemPhysChem* **2002**, *3*, 33 – 42.
[100] S. Hammes-Schiffer, N. Iordanova, *Biochim. Biophys. Acta* **2004**, *1655*, 29 – 36.
[101] A. Soudackov, S. Hammes-Schiffer, *J. Chem. Phys.* **1999**, *111*, 4672 – 4687.
[102] I. Rostov, S. Hammes-Schiffer, *J. Chem. Phys.* **2001**, *115*, 285 – 296.
[103] A. Soudackov, S. Hammes-Schiffer, *J. Chem. Phys.* **2000**, *113*, 2385 – 2396.
[104] E. Hatcher, A. Soudackov, S. Hammes-Schiffer, *J. Phys. Chem. B* **2005**, *109*, 18565 – 18574.
[105] S. Hammes-Schiffer, S. R. Billeter, *Int. Rev. Phys. Chem.* **2001**, *20*, 591 – 616.
[106] "Proton-Coupled Electron Transfer": S. Hammes-Schiffer in *Electron Transfer in Chemistry: Principles, Theories, Methods, and Techniques, Vol. I* (Ed.: V. Balzani), Wiley-VCH, Weinheim, **2001**.
[107] A. Soudackov, E. Hatcher, S. Hammes-Schiffer, *J. Chem. Phys.* **2005**, *122*, 014505.
[108] Y. Georgievskii, A. A. Stuchebrukhov, *J. Chem. Phys.* **2000**, *113*, 10438 – 10450.
[109] G. Villani, *Chem. Phys.* **2004**, *302*, 309 – 322.
[110] S. Shin, S. I. Cho, *Chem. Phys.* **2000**, *259*, 27 – 38.
[111] F. Rappaport, M. Guergova-Kuras, P. J. Nixon, B. A. Diner, J. Lavergne, *Biochemistry* **2002**, *41*, 8518 – 8527.
[112] C. Carra, N. Iordanova, S. Hammes-Schiffer, *J. Am. Chem. Soc.* **2003**, *125*, 10429 – 10436.
[113] M. Sjödin, S. Styring, B. Akermark, L. Sun, L. Hammarström, *J. Am. Chem. Soc.* **2000**, *122*, 3932 – 3936.
[114] E. J. Land, G. Porter, J. Y. Fang, E. Strachan, *Trans. Faraday Soc.* **1961**, *57*, 1885 – 1893.
[115] These values are only approximations to the membrane potentials and neglect ΔG differences for the formation of the Tyr-O$^{\cdot\cdots+}$H-His and Tyr-O–H$\cdots$His H-bonded complexes.
[116] M. Sjödin, S. Styring, H. Wolpher, Y. Xu, L. Sun, L. Hammarström, *J. Am. Chem. Soc.* **2005**, *127*, 3855 – 3863.
[117] L. I. Krishtalik, *Bioelectrochem. Bioenerg.* **1990**, *23*, 249 – 264.
[118] L. I. Krishtalik, *Biochim. Biophys. Acta* **1986**, *849*, 162 – 171.
[119] L. I. Krishtalik, *Biochim. Biophys. Acta* **2003**, *1604*, 13 – 21.
[120] G. Renger, C. Wolff, *Biochim. Biophys. Acta* **1976**, *423*, 610 – 614.
[121] J. Haveman, P. Mathis, *Biochim. Biophys. Acta* **1976**, *440*, 346 – 355.
[122] I. Vass, S. Styring, *Biochemistry* **1991**, *30*, 830 – 839.
[123] M. H. Vos, H. J. Vangorkom, P. J. Vanleeuwen, *Biochim. Biophys. Acta* **1991**, *1056*, 27 – 39.
[124] W. Hillier, T. Wydrzynski, *Biochim. Biophys. Acta* **2001**, *1503*, 197 – 209.
[125] M. Karge, K. D. Irrgang, G. Renger, *Biochemistry* **1993**, *32*, 9772 – 9780.
[126] H. Koike, B. Hanssum, Y. Inoue, G. Renger, *Biochim. Biophys. Acta* **1987**, *893*, 524 – 533.
[127] G. Renger, B. Hanssum, *FEBS Lett.* **1992**, *299*, 28 – 32.
[128] M. Haumann, O. Bogershausen, D. Cherepanov, R. Ahlsbrink, W. Junge, *Photosynth. Res.* **1997**, *51*, 193 – 208.
[129] G. Renger, *Biochim. Biophys. Acta* **2001**, *1503*, 210 – 228.
[130] A. Gelasco, M. L. Kirk, J. W. Kampf, V. L. Pecoraro, *Inorg. Chem.* **1997**, *36*, 1829 – 1837.
[131] J. Bernadou, B. Meunier, *Chem. Commun.* **1998**, 2167 – 2173.
[132] A. Dovletoglou, T. J. Meyer, *J. Am. Chem. Soc.* **1994**, *116*, 215 – 223.
[133] T. J. Meyer, M. H. V. Huynh, *Inorg. Chem.* **2003**, *42*, 8140 – 8160.
[134] M. P. Klein, K. Sauer, V. K. Yachandra, *Photosynth. Res.* **1993**, *38*, 265 – 277.
[135] T.-A. Ono, T. Noguchi, Y. Inoue, M. Kusunoki, T. Matsushita, H. Oyanagi, *Science* **1992**, *258*, 1335 – 1337.
[136] T. A. Roelofs, W. C. Liang, M. J. Latimer, R. M. Cinco, A. Rompel, J. C. Andrews, K. Sauer, V. K. Yachandra, M. P. Klein, *Proc. Natl. Acad. Sci. USA* **1996**, *93*, 3335 – 3340.
[137] M. J. Latimer, H. Dau, W. C. Liang, J. C. Andrews, T. A. Roelofs, R. M. Cinco, A. Rompel, K. Sauer, V. K. Yachandra, M. P. Klein, *Synchrotron Radiat. Tech. Ind. Chem. Mater. Sci.* **1996**, 141 – 148.
[138] L. Iuzzolino, J. Dittmer, W. Dörner, W. Meyer-Klaucke, H. Dau, *Biochemistry* **1998**, *37*, 17112 – 17119.
[139] H. Schiller, J. Dittmer, L. Iuzzolino, W. Dorner, W. Meyer-Klaucke, V. A. Sole, H. F. Nolting, H. Dau, *Biochemistry* **1998**, *37*, 7340 – 7350.
[140] J. Messinger, J. H. Robblee, U. Bergmann, C. Fernandez, P. Glatzel, H. Visser, R. M. Cinco, K. L. McFarlane, E. Bellacchio, S. A. Pizarro, S. P. Cramer, K. Sauer, M. P. Klein, V. K. Yachandra, *J. Am. Chem. Soc.* **2001**, *123*, 7804 – 7820.
[141] U. Bergmann, M. M. Grush, C. R. Horne, P. DeMarois, J. E. Penner-Hahn, C. F. Yocum, D. W. Wright, C. E. Dube, W. H. Armstrong, G. Christou, H. J. Eppley, S. P. Cramer, *J. Phys. Chem. B* **1998**, *102*, 8350 – 8352.
[142] J. M. Peloquin, K. A. Campbell, D. W. Randall, M. A Evanchik, V. L. Pecoraro, W. H. Armstrong R. D. Britt, *J. Am. Chem. Soc.* **2000**, *122*, 10926 – 10942.
[143] P. J. Riggs, R. Mei, C. F. Yocum, J. E. Penner-Hahn, *J. Am. Chem. Soc.* **1992**, *114*, 10650 – 10651.

[144] V. K. Yachandra, *Structure of the Manganese Complex in Photosystem II: Insights from X-ray Spectroscopy*, *Philos. Trans. R. Soc. London Ser. B* **2002**, *357*, 1347 – 1358.
[145] L. V. Kulik, W. Lubitz, J. Messinger, *Biochemistry* **2005**, *44*, 9368 – 9374.
[146] M. A. Strickler, L. M. Walker, W. Hillier, R. J. Debus, *Biochemistry* **2005**, *44*, 8571 – 8577.
[147] J. Yano, J. Kern, K. D. Irrgang, M. J. Latimer, U. Bergmann, P. Glatzel, Y. Pushkar, J. Biesiadka, B. Loll, K. Sauer, J. Messinger, A. Zouni, V. K. Yachandra, *Proc. Natl. Acad. Sci. USA* **2005**, *102*, 12047 – 12052.
[148] V. K. Yachandra, V. J. DeRose, M. J. Latimer, I. Mukerji, K. Sauer, M. P. Klein, *Science* **1993**, *260*, 675 – 679.
[149] R. M. Cinco, J. H. Robblee, J. Messinger, C. Fernandez, K. M. L. Holman, K. Sauer, V. K. Yachandra, *Biochemistry* **2004**, *43*, 13271 – 13282.
[150] J. H. Robblee, R. M. Cinco, V. K. Yachandra, *Biochim. Biophys. Acta* **2001**, *1503*, 7 – 23.
[151] J. H. Robblee, J. Messinger, R. M. Cinco, K. L. McFarlane, C. Fernandez, S. A. Pizarro, K. Sauer, V. K. Yachandra, *J. Am. Chem. Soc.* **2002**, *124*, 7459 – 7471.
[152] J. Yano, Y. Pushkar, P. Glatzel, A. Lewis, K. Sauer, J. Messinger, U. Bergmann, V. K. Yachandra, *J. Am. Chem. Soc.* **2005**, *127*, 14974 – 14975.
[153] J. Yano, J. Kern, K. Sauer, M. J. Latimer, Y. Pushkar, J. Biesiadka, B. Loll, W. Saenger, J. Messinger, A. Zouni, V. K. Yachandra, *Science* **2006**, *314*, 821 – 825.
[154] G. T. Babcock in *Photosynthesis from Light to Biosphere*, *Vol. 2* (Ed.: P. Mathis), Kluwer, Dordrecht, **1995**, p. 209.
[155] C. Tommos, X. S. Tang, K. Warncke, C. W. Hoganson, S. Styring, J. McCracken, B. A. Diner, G. T. Babcock, *J. Am. Chem. Soc.* **1995**, *117*, 10325 – 10335.
[156] N. Ioannidis, J. H. A. Nugent, V. Petrouleas, *Biochemistry* **2002**, *41*, 9589 – 9600.
[157] K. B. Schowen, H. H. Limbach, G. S. Denisov, R. L. Schowen, *Biochim. Biophys. Acta* **2000**, *1458*, 43 – 62.
[158] G. A. Jeffrey, W. Saenger, *Hydrogen Bonding in Biological Structures*, Springer, Berlin, **1991**.
[159] G. A. Jeffrey, *An Introduction to Hydrogen Bonding*, Oxford University Press, New York, **1997**.
[160] S. Scheiner, *Hydrogen Bonding. Theoretical Perspectives*, Oxford University Press, New York, **1997**.
[161] R. F. W. Bader, *Atom in Molecules: A Quantum Theory*, Oxford University Press, New York, **1990**.
[162] S. J. Grabowski, *J. Phys. Org. Chem.* **2004**, *17*, 18 – 31.
[163] M. Hundelt, A.-M. A. Hayes, R. J. Debus, W. Junge, *Biochemistry* **1998**, *37*, 14450 – 14456.
[164] H. J. Eckert, G. Renger, *FEBS Lett.* **1988**, *236*, 425 – 431.
[165] W. Junge, M. Haumann, R. Ahlbrink, A. Mulkidjanian, J. Clausen, *Philos. Trans. R. Soc. London Ser. B* **2002**, *357*, 1407 – 1418.
[166] G. Christen, G. Renger, *Biochemistry* **1999**, *38*, 2068 – 2077.
[167] M. J. Schilstra, F. Rappaport, J. H. A. Nugent, C. J. Barnett, D. R. Klug, *Biochemistry* **1998**, *37*, 3974 – 3981.
[168] A.-M. A. Hays, I. R. Vassiliev, J. H. Golbec, R. J. Debus, *Biochemistry* **1999**, *38*, 11851 – 11865.
[169] C. F. , Baes, Jr., R. E. Messmer, *The Hydrolysis of Metal Cations*, R. E.Kreiger, Malabar, FL, **1986**.
[170] H. B. Gray, J. R. Inkler, *Proc. Natl. Acad. Sci. USA* **2005**, *102*, 3533.
[171] C. C. Oser, J. M. Keske, K. Warncke, R. S. Farid, P. L. Utton, *Nature* **1992**, *355*, 796.
[172] P. M. Kiefer, J. T. Hynes, *J. Phys. Chem. A* **2004**, *108*, 11809 – 11818.
[173] D. P. Mohammed, J. Dreyer, E. Pines, E. T. J. Nibbering, *Science* **2005**, *310*, 83 – 86.
[174] S. Iwata, J. Barber, *Curr. Opin. Struct. Biol.* **2004**, *14*, 447 – 453.
[175] J. Barber, K. Ferreira, K. Maghlaoui, S. Iwata, *Phys. Chem. Chem. Phys.* **2004**, *6*, 4737 – 4742.
[176] J. De Las Rivas, J. Barber, *Photosynth. Res.* **2004**, *81*, 329 – 343.
[177] H. Ishikita, W. Saenger, B. Loll, J. Biesiadka, E.-W. Knapp, *Biochemistry* **2006**, *45*, 2063 – 2071.
[178] H. Ishikita, E.-W. Knapp, *Biochemistry* **2005**, *44*, 14772 – 14783.
[179] D. W. Pipes, M. Bakir, S. E. Vitols, D. J. Hodgson, T. J. Meyer, *J. Am. Chem. Soc.* **1990**, *112*, 5507 – 5514.
[180] S. Saphon, A. R. Crofts, *Z. Naturforsch. C* **1977**, *32*, 617 – 626.
[181] C. F. Fowler, *Biochim. Biophys. Acta* **1977**, *462*, 414 – 421.
[182] V. Förster, W. Junge, *Photochem. Photobiol.* **1985**, *41*, 183 – 190.
[183] J. Lavergne, W. Junge, *Photosynth. Res.* **1993**, *38*, 279 – 296.
[184] M. Haumann, W. Junge, *Oxygenic Photosynthesis: The Light Reactions* (Eds.: D. R. Ort, C. F. Yocum), Kluwer Academic, Dordrecht, **1996**, pp. 165 – 192.
[185] F. Rappaport, J. Lavergne, *Biochemistry* **1991**, *30*, 10004 – 10012.
[186] F. Rappaport, J. Lavergne, *Biochim. Biophys. Acta* **2001**, *1503*, 246 – 259.
[187] U. Wacker, E. Haag, G. Renger, *Curr. Res. Photosynth* **1990**, *1*, A869 – A872.
[188] K. Lübbers, W. Junge, *Curr. Res. Photosynth* **1990**, *1*, 877 – 880.
[189] M. Haumann, W. Junge, *Biochemistry* **1994**, *33*, 864 – 872.
[190] G. Renger, *Photosynthetica* **1987**, *21*, 203 – 224.
[191] B. A. Diner, P. J. Nixon, J. W. Farchaus, *Curr. Opin. Struct. Biol.* **1991**, *1*, 546 – 554.
[192] K. A. Campbell, D. A. Force, P. J. Nixon, F. Dole, B. A. Diner, R. D. Britt, *J. Am. Chem. Soc.* **2000**, *122*, 3754 – 3761.
[193] S. Styring, Y. Feyziyev, F. Mamedov, W. Hillier, G. T. Babcock, *Biochemistry* **2003**, *42*, 6185 – 6192.
[194] R. J. Debus, M. A. Strickler, L. M. Walker, W. Hillier, *Biochemistry* **2005**, *44*, 1367 – 1374.
[195] A. Boussac, A. L. Etienne, *Biochem. Biophys. Res. Commun.* **1982**, *109*, 1200 – 1205.
[196] D. A. Buckingham, A. M. Sargeson, F. P. J. Dwyer, D. P. Mellor, *Chelating agents and metal chelates*, New York, Academic Press, **1964**, chap. 6.
[197] G. A. Heath, K. A. Moock, D. W. A. Sharp, L. J. Yellowlees, *J. Chem. Soc. Chem. Commun.* **1985**, 1503 – 1505.
[198] V. Petrouleas, D. Koulougliotis, N. Ioannidis, *Biochemistry* **2005**, *44*, 6723 – 6728.
[199] G. C. Dismukes, Y. Siderer, *Proc. Natl. Acad. Sci. USA* **1981**, *78*, 274 – 278.
[200] K. A. Åhrling, S. Peterson, S. Styring, *Biochemistry* **1997**, *36*, 13148 – 13152
[201] J. Messinger, J. H. Robblee, W. O. Yu, K. Sauer, V. K. Yachandra, M. P. Klein, *J. Am. Chem. Soc.* **1997**, *119*, 11349 – 11350.
[202] W. P. Jencks, *Catalysis in Chemistry and Enzymology*, McGraw-Hill, New York, **1969**, p. 172.
[203] In water, the equilibrium defining acidity is $HA + H_2O \rightleftharpoons H_3O^+ + A^-$ and $K_a(HA) = (a_{H^+}/a_{H^+}{}^o)\ (a_{A^-}/a_{A^-}{}^o)/(a_{HA}/a_{HA}{}^o)$, in which a_{H^+} etc. are the activities of the components at equilibrium and $a_{H^+}{}^o$ etc. are the activities of the components in their standard states. In dilute solution under ideal conditions, $K_a(HA) = [H_3O^+][A^-]/[HA]$. For the acidity of H_3O^+ in H_2O, $H_3O^+ + H_2O \rightleftharpoons H_3O^+ + H_2O$, $K = 1$. To compare the acidity of H_3O^+ with HA, it is necessary to include the concentration of water in water (55.5 M at 25 °C) with $K_a(H_3O^+) = K[H_3O^+] = 55.5$ M and $pK_a(H_3O^+) = -1.74$. A related argument leads to $pK_a(H_2O) = 15.7$ through the equilibrium $2H_2O \rightleftharpoons H_3O^+ + OH^-$ and $K_w = 10^{-14}$.
[204] T. Noguchi, M. Sugiura, *Biochemistry* **2001**, *40*, 1497 – 1502.
[205] Y. Kimura, T. A. Ono, *Biochemistry* **2001**, *40*, 14061 – 14068.
[206] H. A. Chu, W. Hillier, R. J. Debus, *Biochemistry* **2004**, *43*, 3152 – 3166.

[207] Y. Kimura, N. Mizusawa, T. Yamanari, A. Ishii, T.-A. Ono, *J. Biol. Chem.* **2004**, *280*, 2078 – 2083.
[208] O. Saygin, H. T. Witt, *FEBS Lett.* **1985**, *187*, 224 – 226.
[209] F. Rappaport, M. Blanchard-Desce, J. Lavergne, *Biochim. Biophys. Acta* **1994**, *1184*, 178 – 192.
[210] P. R. Rich, I. D. S. Bendall in *Protein Electron Transfer* (Ed.: D. T. Richens), BIOS Scientific, Oxford, **1997**, pp. 217 – 248.
[211] J. G. Mohanty, A. Chakravorty, *Inorg. Chem.* **1977**, *16*, 1561 – 1563.
[212] J. E. Penner-Hahn, C. F. Yocum, *Science* **2005**, *310*, 982 – 983.
[213] A. S. Denisenko, A. K. Kukushkin, *Biofizika* **2005**, *50*, 833 – 842.
[214] H. Dau, P. Liebisch, M. Haumann, *Anal. Bioanal. Chem.* **2003**, *376*, 562 – 583.
[215] M. Haumann, P. Liebisch, C. Muller, M. Barra, M. Grabolle, H. Dau, *Science* **2005**, *310*, 1019 – 1021.
[216] W. G. Gregor, R. M. Cinco, H. Yu, V. K. Yachandra, R. D. Britt, *Biochemistry* **2005**, *44*, 8817 – 8825.
[217] W. C. Liang, T. A. Roelofs, R. M. Cinco, A. Rompel, M. J. Latimer, W. O. Yu, K. Sauer, M. P. Klein, V. K. Yachandra, *J. Am. Chem. Soc.* **2000**, *122*, 3399 – 3412.
[218] R. D. Guiles, J.-L. Zimmermann, A. E. McDermott, V. K. Yachandra, J. L. Cole, S. L. Dexheimer, R. D. Britt, K. Wieghardt, U. Bossek, K. Sauer, M. P. Klein, *Biochemistry* **1990**, *29*, 471 – 485.
[219] M. Karge, K.-D. Irrgang, G. Renger, *Biochemistry* **1997**, *36*, 8904 – 8913.
[220] M. Haumann, C. Muller, P. Liebisch, L. Iuzzolino, J. Dittmer, M. Grabolle, T. Neisius, W. Meyer-Klaucke, H. Dau, *Biochemistry* **2005**, *44*, 1894 – 1908.
[221] D. Koulougliotis, J. R. Shen, N. Ioannidis, V. Petrouleas, *Biochemistry* **2003**, *42*, 3045 – 3053.
[222] A. Boussac, M. Sugiura, D. Kirilovsky, A. W. Rutherford, *Plant Cell Physiol.* **2005**, *46*, 837 – 842.
[223] J. Messinger, J. H. Robblee, U. Bergmann, C. Fernandez, P. Glatzel, H. Visser, R. M. Cinco, K. L. McFarlane, E. Bellacchio, S. A. Pizarro, S. P. Cramer, K. Sauer, M. P. Klein, V. K. Yachandra, *J. Am. Chem. Soc.* **2001**, *123*, 7804 – 7820.
[224] L. E. Andreasson, I. Vass, S. Styring, *Biochim. Biophys. Acta* **1995**, *1230*, 155 – 164.
[225] A. Boussac, J. L. Zimmermann, A. W. Rutherford, *Biochemistry* **1989**, *28*, 8984 – 8989.
[226] N. Lydakis-Simantiris, P. Dorlet, D. F. Ghanotakis, G. T. Babcock, *Biochemistry* **1998**, *37*, 6427 – 6435.
[227] N. Knoepfle, T. M. Bricker, C. Putnam-Evans, *Biochemistry* **1999**, *38*, 1582 – 1588.
[228] W. Hillier, J. Messinger, T. Wydrzynski, *Biochemistry* **1998**, *37*, 16908 – 16914.
[229] W. Hillier, T. Wydrzynski, *Biochemistry* **2000**, *39*, 4399 – 4405.
[230] G. Hendry, T. Wydrzynski, *Biochemistry* **2002**, *41*, 13328 – 13334.
[231] W. Hillier, T. Wydrzynski, *Phys. Chem. Chem. Phys.* **2004**, *6*, 4882 – 4889.
[232] K. Hasegawa, Y. Kimura, T. A. Ono, *Biochemistry* **2002**, *41*, 13839 – 13850.
[233] P. M. Kelley, S. Izawa, *Biochim. Biophys. Acta* **1978**, *502*, 198 – 210.
[234] K. Lindberg, L. E. Andreasson, *Biochemistry* **1996**, *35*, 14259 – 14267.
[235] H. Yu, C. P. Aznar, X. Xu, R. D. Britt, *Biochemistry* **2005**, *44*, 12022 – 12029.
[236] T. Matsukawa, H. Mino, D. Yoneda, A. Kawamori, *Biochemistry* **1999**, *38*, 4072 – 4077.
[237] R. Razeghifard, R. J. Pace, *Biochemistry* **1999**, *38*, 1252 – 1257.
[238] J. Clausen, W. Junge, *Nature* **2004**, *430*, 480 – 483.
[239] P. E. M. Siegbahn, M. R. A. Blomberg, *Annu. Rev. Phys. Chem.* **1999**, *50*, 221 – 249.
[240] P. E. M. Siegbahn, M. R. A. Blomberg, *Chem. Rev.* **2000**, *100*, 421 – 437.

